ACKNOWLEDGMENTS

Present address for H. Akita: Graduate School of Pharmaceutical Sciences, Hokkaido University, Nishi 6, Kita 12, Kita-ku, Sapporo 060–0812, Japan.

GRANTS

This work was supported by Scientific Research on Priority Areas Epithelial Vectorial Transport Grant-in-Aid 12144201 and a grant-in-aid for Center of Excellence from The Ministry of Education, Culture, Sports, Science and Technology of Japan.

REFERENCES

1. **Akita H, Suzuki H, Ito K, Kinoshita S, Sato N, Takikawa H, and Sugiyama Y.** Characterization of bile acid transport mediated by multidrug resistance associated protein 2 and bile salt export pump. *Biochim Biophys Acta* 1511: 7–16, 2001.
2. **Akita H, Suzuki H, and Sugiyama Y.** Sinusoidal efflux of taurocholate correlates with the hepatic expression level of Mrp3. *Biochem Biophys Res Commun* 299: 681–687, 2002.
3. **Boyer JL, Ng OC, Ananthanarayanan M, Hofmann AF, Schteingart CD, Hagenbuch B, Stieger B, and Meier PJ.** Expression and characterization of a functional rat liver Na^+ bile acid cotransport system in COS-7 cells. *Am J Physiol Gastrointest Liver Physiol* 266: G382–G387, 1994.
4. **Byrne JA, Strautnieks SS, Mieli-Vergani G, Higgins CF, Linton KJ, and Thompson RJ.** The human bile salt export pump: characterization of substrate specificity and identification of inhibitors. *Gastroenterology* 123: 1649–1658, 2002.
5. **Cui Y, Konig J, Buchholz JK, Spring H, Leier I, and Keppler D.** Drug resistance and ATP-dependent conjugate transport mediated by the apical multidrug resistance protein, MRP2, permanently expressed in human and canine cells. *Mol Pharmacol* 55: 929–937, 1999.
6. **Cui Y, Konig J, and Keppler D.** Vectorial transport by double-transfected cells expressing the human uptake transporter SLC21A8 and the apical export pump ABCC2. *Mol Pharmacol* 60: 934–943, 2001.
7. **Gerloff T, Stieger B, Hagenbuch B, Madon J, Landmann L, Roth J, Hofmann AF, and Meier PJ.** The sister of P-glycoprotein represents the canalicular bile salt export pump of mammalian liver. *J Biol Chem* 273: 10046–10050, 1998.
8. **Goh LB, Spears KJ, Yao D, Ayrton A, Morgan P, Roland Wolf C, and Friedberg T.** Endogenous drug transporters in in vitro and in vivo models for the prediction of drug disposition in man. *Biochem Pharmacol* 64: 1569–1578, 2002.
9. **Green RM, Hoda F, and Ward KL.** Molecular cloning and characterization of the murine bile salt export pump. *Gene* 241: 117–123, 2000.
10. **Hagenbuch B and Meier PJ.** Molecular cloning, chromosomal localization, and functional characterization of a human liver Na^+/bile acid cotransporter. *J Clin Invest* 93: 1326–1331, 1994.
11. **Hagenbuch B, Stieger B, Foguet M, Lubbert H, and Meier PJ.** Functional expression cloning and characterization of the hepatocyte Na^+/bile acid cotransport system. *Proc Natl Acad Sci USA* 88: 10629–10633, 1991.
12. **Hasegawa M, Kusuhara H, Sugiyama D, Ito K, Ueda S, Endou H, and Sugiyama Y.** Functional involvement of rat organic anion transporter 3 (rOat3; Slc22a8) in the renal uptake of organic anions. *J Pharmacol Exp Ther* 300: 746–753, 2002.
13. **Keppler D and Konig J.** Hepatic secretion of conjugated drugs and endogenous substances. *Semin Liver Dis* 20: 265–272, 2000.
14. **Konig J, Nies AT, Cui Y, Leier I, and Keppler D.** Conjugate export pumps of the multidrug resistance protein (MRP) family: localization, substrate specificity, and MRP2-mediated drug resistance. *Biochim Biophys Acta* 1461: 377–394, 1999.
15. **Kouzuki H, Suzuki H, Ito K, Ohashi R, and Sugiyama Y.** Contribution of sodium taurocholate co-transporting polypeptide to the uptake of its possible substrates into rat hepatocytes. *J Pharmacol Exp Ther* 286: 1043–1050, 1998.
16. **Lowry OH, Rosebrough NJ, Farr AL, and Randall RJ.** Protein measurement with the Folin phenol reagent. *J Biol Chem* 193: 265–275, 1951.
17. **Meier PJ, Eckhardt U, Schroeder A, Hagenbuch B, and Stieger B.** Substrate specificity of sinusoidal bile acid and organic anion uptake systems in rat and human liver. *Hepatology* 26: 1667–1677, 1997.
18. **Meier PJ and Stieger B.** Bile salt transporters. *Annu Rev Physiol* 64: 635–661, 2002.
19. **Mizuguchi H and Kay MA.** Efficient construction of a recombinant adenovirus vector by an improved in vitro ligation method. *Hum Gene Ther* 9: 2577–2583, 1998.
20. **Mizuguchi H and Kay MA.** A simple method for constructing E1- and E1/E4-deleted recombinant adenoviral vectors. *Hum Gene Ther* 10: 2013–2017, 1999.
21. **Ng KH, Lim BG, and Wong KP.** Sulfate conjugating and transport functions of MDCK distal tubular cells. *Kidney Int* 63: 976–986, 2003.
22. **Niwa H, Yamamura K, and Miyazaki J.** Efficient selection for high-expression transfectants with a novel eukaryotic vector. *Gene* 108: 193–199, 1991.
23. **Noe J, Stieger B, and Meier PJ.** Functional expression of the canalicular bile salt export pump of human liver. *Gastroenterology* 123: 1659–1666, 2002.
24. **Platte HD, Honscha W, Schuh K, and Petzinger E.** Functional characterization of the hepatic sodium-dependent taurocholate transporter stably transfected into an immortalized liver-derived cell line and V79 fibroblasts. *Eur J Cell Biol* 70: 54–60, 1996.
25. **Rius M, Nies AT, Hummel-Eisenbeiss J, Jedlitschky G, and Keppler D.** Cotransport of reduced glutathione with bile salts by MRP4 (ABCC4) localized to the basolateral hepatocyte membrane. *Hepatology* 38: 374–384, 2003.
26. **Sasaki M, Suzuki H, Ito K, Abe T, and Sugiyama Y.** Transcellular transport of organic anions across a double-transfected Madin-Darby canine kidney II cell monolayer expressing both human organic anion-transporting polypeptide (OATP2/SLC21A6) and multidrug resistance-associated protein 2 (MRP2/ABCC2). *J Biol Chem* 277: 6497–6503, 2002.
27. **Schroeder A, Eckhardt U, Stieger B, Tynes R, Schteingart CD, Hofmann AF, Meier PJ, and Hagenbuch B.** Substrate specificity of the rat liver Na^+-bile salt cotransporter in *Xenopus laevis* oocytes and in CHO cells. *Am J Physiol Gastrointest Liver Physiol* 274: G370–G375, 1998.
28. **Shi X, Bai S, Ford AC, Burk RD, Jacquemin E, Hagenbuch B, Meier PJ, and Wolkoff AW.** Stable inducible expression of a functional rat liver organic anion transport protein in HeLa cells. *J Biol Chem* 270: 25591–25595, 1995.
29. **Sorscher S, Lillienau J, Meinkoth JL, Steinbach JH, Schteingart CD, Feramisco J, and Hofmann AF.** Conjugated bile acid uptake by *Xenopus laevis* oocytes induced by microinjection with ileal Poly A+ mRNA. *Biochem Biophys Res Commun* 186: 1455–1462, 1992.
30. **Stieger B, Fattinger K, Madon J, Kullak-Ublick GA, and Meier PJ.** Drug- and estrogen-induced cholestasis through inhibition of the hepatocellular bile salt export pump (Bsep) of rat liver. *Gastroenterology* 118: 422–430, 2000.
31. **Stieger B, Hagenbuch B, Landmann L, Hochli M, Schroeder A, and Meier PJ.** In situ localization of the hepatocytic Na^+/taurocholate cotransporting polypeptide in rat liver. *Gastroenterology* 107: 1781–1787, 1994.
32. **Suzuki H and Sugiyama Y.** Excretion of GSSG and glutathione conjugates mediated by MRP1 and cMOAT/MRP2. *Semin Liver Dis* 18: 359–376, 1998.
33. **Trauner M and Boyer JL.** Bile salt transporters: molecular characterization, function, and regulation. *Physiol Rev* 83: 633–671, 2003.
34. **Yamaoka K, Tanigawara Y, Nakagawa T, and Uno T.** A pharmacokinetic analysis program (multi) for microcomputer. *J Pharmacobio-Dyn* 4: 879–885, 1981.

0090-9556/05/3310-1477–1481$20.00
DRUG METABOLISM AND DISPOSITION
Copyright © 2005 by The American Society for Pharmacology and Experimental Therapeutics
DMD 33:1477–1481, 2005

Vol. 33, No. 10
4622/3053559
Printed in U.S.A.

CONTRIBUTION OF OATP (ORGANIC ANION-TRANSPORTING POLYPEPTIDE) FAMILY TRANSPORTERS TO THE HEPATIC UPTAKE OF FEXOFENADINE IN HUMANS

Maki Shimizu, Kaori Fuse, Kazuho Okudaira, Ryuichiro Nishigaki, Kazuya Maeda, Hiroyuki Kusuhara, and Yuichi Sugiyama

Faculty of Pharmaceutical Sciences, Toho University, Chiba, Japan (M.S., K.F., K.O., R.N.); and Graduate School of Pharmaceutical Sciences, the University of Tokyo, Tokyo, Japan (K.M., H.K., Y.S.)

Received March 7, 2005; accepted July 12, 2005

ABSTRACT:

Fexofenadine hydrochloride (FEX), a second generation H_1-receptor antagonist, is mainly eliminated from the liver into bile in unchanged form. Recent studies have shown that FEX can be accepted by human MDR1 (P-glycoprotein), OATP1A2 [organic anion-transporting polypeptide (OATP)-A, and OATP2B1 (OATP-B)] expression systems. However, other transporters responsible for the hepatic uptake of FEX have not yet been identified. In the present study, we evaluated the contribution of OATP family transporters, namely OATP1B1 (OATP2/OATP-C), OATP1B3 (OATP8), and OATP2B1 (OATP-B), to FEX uptake using transporter-expressing HEK293 (human embryonic kidney) cells. The uptake of FEX in OATP1B3-expressing cells was significantly greater than that in vector-transfected cells. On the other hand, OATP1B1- or OATP2B1-mediated uptake of FEX was not statistically significant. OATP1B3-mediated transport could be explained by a one-saturable component with a Michaelis constant (K_m) of 108 ± 11 μM. The inhibitory effect of FEX on the uptake of estrone-3-sulfate (E_1S), cholecystokinin octapeptide (CCK-8), and 17β-estradiol-17β-D-glucuronide ($E_2$17βG) was also examined. Both OATP1B1- and OATP1B3-mediated $E_2$17βG uptake was inhibited by FEX. The K_i values were 148 ± 61 and 205 ± 72 μM for OATP1B1 and OATP1B3, respectively. FEX also inhibited OATP1B3-mediated CCK-8 uptake and OATP1B1-mediated E_1S uptake with a K_i value of 83.3 ± 15.3 and 257 ± 84 μM, respectively, suggesting that FEX could not be used as a specific inhibitor for OATP1B1 and OATP1B3, although FEX was preferentially accepted by OATP1B3. In conclusion, this is, to our knowledge, the first demonstration that OATP1B3 is thought to be a major transporter involved in hepatic uptake of FEX in humans.

Several members of different uptake transporter families are thought to be involved in the hepatic uptake of substances in human liver. Since the uptake of substances from blood into hepatocytes is the first step in the hepatocellular elimination, it is increasingly recognized that uptake transporters in the basolateral membrane play an important role in substrate disposition. Organic anion-transporting polypeptides (OATPs) form a superfamily of the sodium-independent transport system that mediates the transmembrane transport of a wide range of amphiphilic organic compounds including bile salts, organic dyes, steroid conjugates, thyroid hormones, anionic oligopeptides, and many drugs, such as pravastatin (Hagenbuch and Meier, 2004).

Fexofenadine hydrochloride (FEX) (Aventis Pharmaceuticals, Inc., Kansas City, MO), a selective histamine H_1-receptor antagonist, is clinically effective in the treatment of seasonal allergic rhinitis and chronic idiopathic urticaria, for which it is considered as first-line therapy (Markham and Wagstaff, 1998; Simpson and Jarvis, 2000). FEX is the active metabolite of terfenadine (Seldane) and FEX showed no significant effect on the prolongation of the corrected QT interval (QT_c) in contrast to terfenadine (Pratt et al., 1999). After oral administration of [^{14}C]FEX (60 mg), most of the total dose was recovered in the urine (12%) and feces (80%), with the majority of the dose (>85%) recovered as the unchanged form (Lippert et al., 1996). This shows that metabolism is an insignificant elimination route and that FEX is poorly absorbed and/or is mainly eliminated from the liver into bile in its unchanged form.

Hepatic metabolism is of minimal importance in the elimination of FEX. On the other hand, coadministration of erythromycin (500 mg three times a day) or ketoconazole (400 mg once daily) with FEX resulted in substantial increase in steady-state plasma concentration of FEX and its plasma AUC by 109 and 164%, respectively (product information, Aventis Pharmaceuticals, Inc.). However, a regional perfusion study showed that ketoconazole did not have a significant effect on the in vivo intestinal absorption of FEX when coadministered or given as a pretreatment (Tannergren et al., 2003).

FEX was shown to be a substrate of P-glycoprotein and OATP1A2 (OATP-A), and its disposition was altered in *mdr1a* (−/−) mice (Cvetkovic et al., 1999). In addition, rifampin increased the oral clearance of FEX, suggesting an up-regulation of P-glycoprotein and, possibly, other transport processes (Hamman et al., 2001). Currently, several OATP family transporters such as OATP1B1 (OATP2/OATP-C), OATP1B3 (OATP8), and OATP2B1 (OATP-B) have been identified on the basal membrane of human liver (Konig et al., 2000a,b;

Article, publication date, and citation information can be found at http://dmd.aspetjournals.org.
doi:10.1124/dmd.105.004622.

ABBREVIATIONS: OATP, organic anion-transporting polypeptide; HEK, human embryonic kidney; AUC, area under the plasma concentration curve; FEX, fexofenadine hydrochloride; E_1S, estrone-3-sulfate; CCK-8, cholecystokinin octapeptide; $E_2$17βG, 17β-estradiol-17β-D-glucuronide; LC/MS, liquid chromatography/mass spectrometry.

Kullak-Ublick et al., 2001). OATP1A2- and OATP2B1-mediated uptake of FEX had been determined previously (Cvetkovic et al., 1999; Nozawa et al., 2004); however, other transporters responsible for the hepatic uptake of FEX have not yet been investigated, and their clinical relevance has not yet been determined.

In this study, we especially focused on the involvement of OATP1B1 and OATP1B3 in the hepatic uptake of FEX because they are exclusively expressed in liver and exhibit similar broad substrate specificities, which suggests that they play a crucial role in the hepatic uptake of several anionic endogenous compounds and drugs (Ismair et al., 2003; Hagenbuch and Meier, 2004).

The substrate specificity of OATP1B3 commonly overlaps that of OATP1B1 (Ismair et al., 2001; Kullak-Ublick et al., 2001). However, there are some differences as far as their substrate recognition and transcriptional regulation are concerned (Hagenbuch and Meier, 2003; Kullak-Ublick et al., 2004). Therefore, it is important to estimate the relative contribution of OATP1B1 and OATP1B3 to the hepatic uptake in humans separately. Recently, two kinds of methodologies were established to identify a quantitative contribution of OATP1B1 and OATP1B3 to the overall hepatic uptake. One is to compare the uptake clearance of transporter-selective compounds in transporter-expressing HEK293 cells and human cryopreserved hepatocytes, and the other is to compare the relative expression level of each transporter in expression system and hepatocytes estimated by Western blot analysis. (Hirano et al., 2004).

In the present study, we evaluated the contribution of OATP1B1 and OATP1B3 to FEX uptake using transporter-expressing HEK293 cells. We also examined the inhibitory effect of FEX on the uptake of a number of reference compounds, which are estrone-3-sulfate (E_1S), a selective substrate of OATP1B1; CCK-8, a selective substrate of OATP1B3; and 17β-estradiol-17β-D-glucuronide ($E_2 17\beta G$), a substrate of both transporters.

Materials and Methods

Materials. FEX was a gift from Aventis Pharmaceuticals, Inc. (Kansas City, MO). [^{3}H]E_1S (57.3 Ci/mmol) and [^{3}H]$E_2 17\beta G$ (45.0 Ci/mmol) were purchased from PerkinElmer Life and Analytical Sciences (Boston, MA). [^{3}H]CCK-8 (68.0 Ci/mmol) was purchased from GE Healthcare (Little Chalfont, Buckinghamshire, UK). Unlabeled E_1S, CCK-8, and $E_2 17\beta G$ were purchased from Sigma (St. Louis, MO). All other chemicals were of analytical grade and commercially available.

Construction of Stably Transfected HEK293 Cells Expressing Human OATP2B1. The human OATP2B1 gene was isolated by polymerase chain reaction using ATCC IMAGE clone (I.D. 5752976) purchased from Summit Pharmaceuticals International Corp. (Tokyo, Japan). To obtain the full-length cDNA of the OATP2B1 gene, pCMV-SPORT6 vector containing OATP2B1 cDNA was digested with EcoRI and NotI. Then, cDNA fragment was ligated into EcoRI and NotI sites of the pcDNA3.1 (+) (Invitrogen, Carlsbad, CA). OATP2B1-expressing HEK293 cells were constructed by the transfection of expression vector into cells using FuGENE6 (Roche Diagnostics, Indianapolis, IN), according to the manufacturer's instruction and selection by 800 μg/ml of the antibiotic G418 sulfate (Promega, Madison, WI) for 3 weeks.

Cell Culture. Transporter-expressing or vector-transfected HEK293 cells were grown in Dulbecco's modified Eagle's medium low glucose (Invitrogen) supplemented with 10% fetal bovine serum (Cansera International Inc., Toronto, ON, Canada), 100 U/ml penicillin, 100 μg/ml streptomycin, and 0.25 μg/ml amphotericin B at 37°C with 5% CO_2 and 95% humidity. Cells were then seeded in 12-well plates (coated with 50 mg/l poly(L-lysine) and 50 mg/l poly(L-ornithine); Sigma) at a density of 1.5×10^5 cells/well. For the transport study, the cell culture medium was replaced with culture medium supplemented with 5 mM sodium butyrate 24 h before transport assay to induce the expression of transporters.

Transport Study Using Transporter Expression Systems. The transport study was carried out as described previously (Hirano et al., 2004). After cells had been washed twice and preincubated with Krebs-Henseleit buffer at 37°C for 15 min, uptake was initiated by adding Krebs-Henseleit buffer containing radiolabeled and unlabeled substrates. The Krebs-Henseleit buffer consisted of 118 mM NaCl, 23.8 mM $NaHCO_3$, 4.8 mM KCl, 1.0 mM KH_2PO_4, 1.2 mM $MgSO_4$, 12.5 mM HEPES, 5.0 mM D-glucose, and 1.5 mM $CaCl_2$ adjusted to pH 7.4. For inhibition studies, inhibitor was added in the incubation buffer. At designated times, the incubation buffer was removed and uptake was terminated by adding ice-cold Krebs-Henseleit buffer. Then, cells were washed twice with 1 ml of ice-cold Krebs-Henseleit buffer and lysed with 500 μl of 0.2 N NaOH overnight at 4°C. Then, 250 μl of 0.4 N HCl was added to the cell lysate and aliquots (500 μl) were transferred to scintillation vials. The radioactivity associated with the cells and incubation buffer was measured in a liquid scintillation counter (LS6500; Beckman Coulter, Fullerton, CA) after adding 2 ml of scintillation fluid (Clear-sol-I; Nacalai Tesque, Kyoto, Japan) to the scintillation vials. The cellular protein amount was determined by the Lowry method using 50 μl of lysate with bovine serum albumin as a standard.

When using FEX as a substrate, aliquots (150 μl) of lysates were transferred to microtubes, mixed with 30 μl of 1 N HCl and 300 μl of 2 ng/ml midazolam (internal standard of LC/MS) in methanol, and deproteinized by centrifugation for 10 min at 13,000 rpm. Then, 50 μl of the supernatants were used for LC/MS analysis.

LC/MS Analysis. FEX concentrations were determined by high-performance liquid chromatography with electrospray mass spectrometry (LC/MS) using the modified protocol described in the previous report (Hofmann et al., 2002). The LC/MS system was operated by MassLynx and QuanLynx software (Waters, Milford, MA). The contents of the mobile phase for high-performance liquid chromatography were 0.05% formic acid in water (A) and methanol (B). Chromatographic separation was achieved on a Capcell Pak C18 MG analytical column (4.6 mm i.d. × 75 mm; particle size 3 μm; Shiseido, Tokyo, Japan) kept at 30°C, using a linear gradient from 55% B to 70% B over 5 min, and a flow rate of 0.8 ml/min. Electrospray parameters were as follows: capillary voltage, 3.10 kV; cone voltage, 50.00 kV; extractor voltage, 5.00 V; source temperature, 100°C; cone temperature, 20°C; desolvation temperature, 350°C; cone gas flow, 50 l/h; and desolvation gas flow, 300 l/h. The mass spectrometer (ZQ 2000 MS detection; Waters) was operated in the selected ion monitoring mode using the respective positive ions, *m/z* 502.30 for FEX and *m/z* 326.10 for midazolam (internal standard). The retention time of FEX was approximately 3.3 min. Standard curves were linear over the range of 2.5~100 nM. The coefficient of variation (CV) of the interassay variability (n = 14; quality controls containing 10 nM FEX) ranged between 3.6 and 11.8%. The CV of the intra-assay variability (n = 9) ranged between 4.7 and 9.8%.

Data Analysis. Kinetic analysis was carried out as described previously (Hirano et al., 2004). Ligand uptake was expressed as the uptake volume (μl/mg protein), given as the amount of radioactivity associated with the cells (dpm/mg protein) divided by its concentration in the incubation medium (dpm/μl). In the case of FEX, ligand uptake (μl/mg protein) was given as the amount of FEX associated with the cells (pmol/mg protein) divided by its concentration in the incubation medium (pmol/μl). Specific uptake was obtained by subtracting the uptake into vector-transfected cells from that into cDNA-transfected cells. Kinetic parameters were obtained using the following equation:

$$v_o = (V_{max} \times S)/(K_m + S) \quad (1)$$

where v_o is the initial uptake rate of substrate (pmol/min/mg protein), S is the substrate concentration in the medium (μM), K_m is the Michaelis constant (μM), and V_{max} is the maximum uptake rate (pmol/min/mg protein). To obtain kinetic parameters, the data were fitted to eq. 1 by a nonlinear least-squares method using the MULTI program (Yamaoka et al., 1981).

The inhibition constant (K_i) of FEX for the uptake of radiolabeled compounds was obtained by fitting the following equation to the data as described previously (Chu et al., 1997):

$$V_{(+I)}/V_{(-I)} = 1/[1 + (I/K_i)] \quad (2)$$

where $V_{(+I)}$ and $V_{(-I)}$ represent the transport velocity in the presence and absence of inhibitor, respectively, and I is the inhibitor concentration. This equation was derived based on two assumptions: the mode of inhibition was competitive or noncompetitive and the concentration of substrates (0.1 μM) used was much lower than their K_m values.

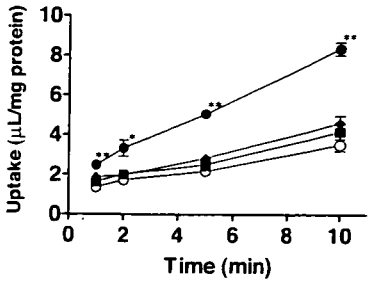

FIG. 1. Time-dependent uptake of FEX in OATP1B1, OATP1B3, and OATP2B1-expressing HEK293 cells. Uptake of FEX (10 μM) was measured for 1, 2, 5, and 10 min using HEK293 cells expressing OATP1B1 (◆), OATP1B3 (●), OATP2B1 (■), or vector-transfected cells (control; ○). Data are shown as the mean ± S.E. of three to eight independent experiments, and each experiment was performed in triplicate. The asterisks represent a statistically significant difference from uptake in the control cell shown by a paired Student's *t* test (*, $p < 0.05$; **, $p < 0.005$).

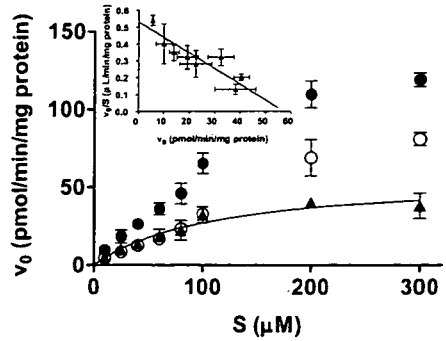

FIG. 2. Concentration-dependence of the OATP1B3-mediated uptake of FEX. Uptake of FEX was measured for 5 min using HEK293 cells expressing OATP1B3 (●) or vector-transfected cells (control; ○). OATP1B3-mediated uptake (▲) was calculated by subtracting the uptake in control cells from that in OATP1B3 cells. Kinetic parameters were obtained by fitting the data for OATP1B3-mediated uptake to the Michaelis-Menten equation (eq. 1) by nonlinear least-squares analysis. The inset is an Eadie-Hofstee plot of the same data. Data are shown as the mean ± S.E. of three to four independent experiments, and each experiment was performed in triplicate.

Statistical Analysis. Statistical differences were determined using a paired Student's *t* test and differences were considered significant at $P < 0.05$.

Results

Uptake of FEX by Transporter-Expressing Cells. To evaluate whether FEX was a substrate for OATP1B1, OATP1B3, or OATP2B1, the uptake of FEX (10 μM) was investigated using OATP1B1-, OATP1B3-, and OATP2B1-expressing cells and vector-transfected HEK293 cells (control). The hepatic uptake clearances of probe substrates $E_2$17βG by OATP1B1, CCK-8 by OATP1B3, and E_1S by OATP2B1 were 14.9 ± 0.3, 5.52 ± 0.28, and 10.8 ± 1.0 μl/min/mg protein, respectively (data not shown). The uptake of FEX in OATP1B3-expressing cells was significantly greater than that in vector-transfected cells ($P < 0.005$) (Fig. 1). Its uptake clearance, which was calculated by the difference in the slope of uptake amount at 1 min and 10 min in expression system and vector-control cells, was 0.409 ± 0.056 μl/min/mg protein. On the other hand, OATP1B1- and OATP2B1-mediated uptake of FEX was only slightly observed, although not statistically significant. The uptake clearance by OATP1B1 and OATP2B1 was 0.0622 ± 0.0586 and 0.0414 ± 0.0614 μl/min/mg protein, respectively (Fig. 1).

The concentration-dependent uptake of FEX was studied using OATP1B3-expressing cells and vector-transfected HEK293 cells. Kinetic analysis revealed that the OATP1B3-mediated uptake of FEX was saturable with a K_m of 108 ± 11 μM and a V_{max} of 56.7 ± 3.2 pmol/min/mg protein (Fig. 2).

Effect of FEX on the Uptake of [^{3}H]E_1S, [^{3}H]CCK-8, and [^{3}H]$E_2$17βG by Transporter-Expressing Cells. The effect of FEX on the uptake of [^{3}H]E_1S and [^{3}H]CCK-8 by transporter-expressing cells is shown in Fig. 3. OATP1B3-mediated CCK-8 uptake was inhibited by FEX (Fig. 3B), whereas OATP1B1-mediated E_1S uptake was weakly inhibited by FEX (Fig. 3A). The K_i values were 257 ± 84 and 83.3 ± 15.3 μM for OATP1B1-mediated E_1S uptake and OATP1B3-mediated CCK-8 uptake, respectively.

The effect of FEX on the uptake of [^{3}H]$E_2$17βG by transporter-expressing cells is shown in Fig. 4. In this case, the K_i values were 148 ± 61 μM for OATP1B1 and 205 ± 72 μM for OATP1B3, respectively.

Discussion

In the present study, we have shown that FEX is efficiently transported by OATP1B3 in human liver, whereas OATP1B1 did not transport FEX significantly. Hirano et al. (2004) have recently established a method for determining the contribution of OATP1B1 and OATP1B3 to the overall hepatic uptake of compounds.

Following one of those approaches, we estimated the relative expression level of OATP1B1 and OATP1B3 in transporter-expression systems and human hepatocytes by using transporter-selective ligands. We found previously that E_1S can be used as an OATP1B1-selective ligand, whereas CCK-8 is an OATP1B3-selective ligand. As shown in the results, we measured the uptake clearance of $E_2$17βG in OATP1B1-expressing cells and CCK-8 in OATP1B3-expressing cells. As for OATP1B1, we can estimate the uptake clearance of E_1S in our expression systems [124 μl/min/mg protein (= 132*14.9/15.8)] by comparing the uptake of $E_2$17βG in our cells (14.9 μl/min/mg protein) with that previously reported (15.8 μl/min/mg protein) (Hirano et al., 2004). Then, following the method as described previously (Hirano et al., 2004), the ratio of the uptake clearance of reference compounds in each batch of human hepatocytes to that in the OATP1B1- and OATP1B3-expression system ($R_{act,\ OATP1B1}$ and $R_{act,\ OATP1B3}$) was found to be 0.887 and 1.43 for lot OCF, 1.08 and 0.634 for lot 094, and 0.465 and 0.366 for lot ETR, respectively. Therefore, we can estimate the predicted uptake clearance of FEX mediated by a specific transporter by multiplying R_{act} by the uptake clearance of FEX in each expression system. If the contribution of OATP1B1 to the hepatic uptake of FEX is assumed to be equal to that of OATP1B3, the following equation should be satisfied:

$$R_{act,\ OATP1B1} \times CL_{OATP1B1,\ fex} = R_{act,\ OATP1B3} \times CL_{OATP1B3,\ fex} \quad (3)$$

where $CL_{OATP1B1,\ fex}$ and $CL_{OATP1B3,\ fex}$ represent the uptake clearance of FEX in our OATP1B1- and OATP1B3-expressing cells. Assuming that OATP1B1 is more important than OATP1B3 in the hepatic uptake of FEX, $CL_{OATP1B1,\ fex}$ should be 1.61-, 0.587-, and 0.787-fold larger than $CL_{OATP1B3,\ fex}$ in lot OCF, 094, and ETR, respectively. However, in Fig. 1, OATP1B1-mediated uptake was less than half the OATP1B3-mediated uptake. This finding suggests that the contribution of OATP1B3 is at least more than 50% of the overall hepatic uptake of FEX.

We showed that OATP2B1 does not transport FEX significantly, although slight enhancement of its uptake by OATP2B1 could be observed (Fig. 1). This is not consistent with a previous result demonstrating the uptake of FEX in OATP2B1-expressing cells at both pH 5.0 and 7.4 (Nozawa et al., 2004). This discrepancy might be due to the low level of OATP2B1 in our expression system, compared with their cells, because the uptake clearance of E_1S at pH 7.4 in our cells (10.8 ± 1.0 μl/min/mg protein) was smaller than that reported previously (Nozawa et al., 2004).

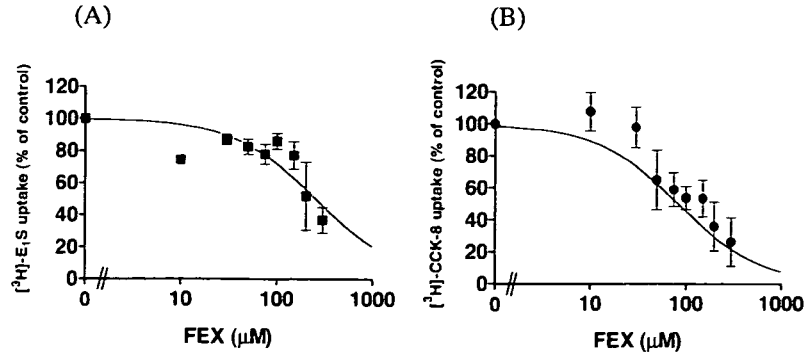

FIG. 3. Inhibitory effect of FEX on the OATP1B1-mediated uptake of E_1S (A) and OATP1B3-mediated uptake of CCK-8 (B). OATP1B1-mediated uptake of [^{3}H]E_1S (A) or OATP1B3-mediated [^{3}H]CCK-8 (B) was calculated by subtracting the uptake in control cells from that in transporter-expressing cells. The concentration of E_1S or CCK-8 was set at 0.1 μM. The inhibition constant (K_i) of FEX for the transporter-mediated uptake was obtained by fitting to eq. 2 using nonlinear least-squares analysis, and the solid line represents the fitted line. Data are shown as the mean ± S.E. of three independent experiments, and each experiment was performed in triplicate.

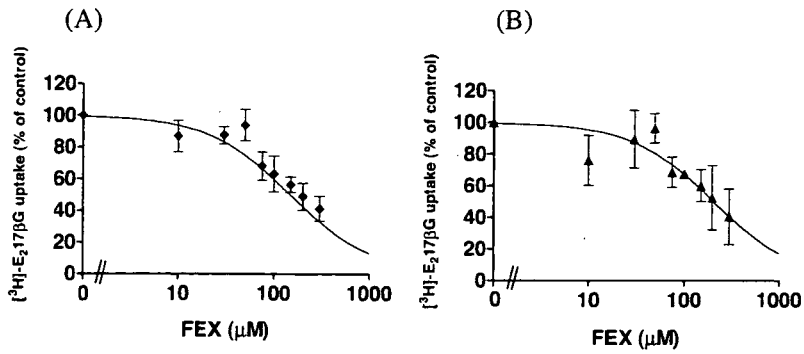

FIG. 4. Inhibitory effect of FEX on the uptake of OATP1B1 (A)- or OATP1B3 (B)-mediated uptake of [^{3}H]$E_2$17βG. OATP1B1 (A)- or OATP1B3 (B)-mediated uptake of $E_2$17βG was calculated by subtracting that in control cells from that in OATP1B1- or OATP1B3-expressing cells (◆, OATP1B1; ▲, OATP1B3). The concentration of $E_2$17βG was set at 0.1 μM. The inhibition constant (K_i) of FEX for the OATP1B1- or OATP1B3-mediated uptake of $E_2$17βG was obtained by fitting to eq. 2 using nonlinear least-squares analysis, and the solid line represents the fitted line. Data are shown as the mean ± S.E. of three independent experiments, and each experiment was performed in triplicate.

Kobayashi et al. (2003) have demonstrated that OATP2B1 is localized on the apical membrane of human intestine, and Nozawa et al. (2003) showed pH-dependent uptake of some organic anions in OATP2B1-expressing cells. In addition, Satoh et al. (2005) have indicated that citrus juice can inhibit the OATP2B1-mediated uptake of anionic compounds, which is consistent with the clinical report showing that fruit juices decreased the bioavailability of FEX in humans (Dresser et al., 2002). Therefore, OATP2B1 might be involved in the intestinal absorption of FEX. On the other hand, we found that the ratio of expression level of OATP2B1 in human hepatocytes per 10^6 cells to that in our transporter expression system per milligram of cellular protein was about 5 times lower than that of OATP1B1 and OATP1B3 (M. Hirano, K. Maeda, Y. Shitara, and Y. Sugiyama, unpublished observation), suggesting that OATP2B1 does not play a major role in the hepatic uptake of FEX, even though it is a substrate for ATP2B1.

We also examined the effect of FEX on the OATP1B1- or OATP1B3-mediated uptake of probe substrates (Figs. 3 and 4). FEX inhibited both OATP1B1- and OATP1B3-mediated uptake of the three compounds we tested. The substrate-dependence of the K_i values was not clearly observed. These inhibitory effects are not likely to be clinically significant because the K_i values were much higher than the reported C_{max} of FEX (459 nM, product information). The inhibitory effect of FEX for OATP1B1 was slightly weaker than that for OATP1B3. The results suggest that FEX was not a specific inhibitor for OATP1B1 or OATP1B3, although it is thought to be a selective substrate for OATP1B3 in human liver.

OATP1B3 shares 80% amino acid identity with OATP1B1, and the spectrum of substrates of OATP1B3 is similar to that of OATP1B1 (Kullak-Ublick et al., 2001). Both OATP1B1 and OATP1B3 have broad substrate specificities, including bile salts (glycocholate, taurocholate), hormones and their conjugates [dehydroepiandrosterone sulfate, $E_2$17βG, thyroid hormones (T3 and T4), leukotriene C_4), peptides [cyclo(L-Leu-D-Trp-D-Asp-L-Pro-D-Val) (BQ-123), [D-Pen^{2,5}]-enkephalin (DPDPE)], drugs (methotrexate, rifampicin), other organic anions (monoglucuronosyl bilirubin, bromosulfophthalein), and natural toxins (microcystin, phalloidin) (Hagenbuch and Meier, 2003). To characterize the contribution of OATP1B3, it is necessary to identify the specific substrate(s) or inhibitor(s) of OATP1B3. Previously, only a few unique substrates for OATP1B3 have been reported, such as CCK-8 (intestinal peptide) (Ismair et al., 2001), deltorphin II (opioid peptide), and digoxin (cardiac glycoside) (Kullak-Ublick et al., 2001) in transporter-expressing *Xenopus laevis* oocytes. However, considering the direct evaluation of the function of OATP1B3 in humans by measuring the hepatic clearance of probe drugs, they cannot be easily used as a clinically applicable probe drug in humans because of the narrow safety margin. In this study, we demonstrated for the first time that FEX may also be a relatively selective substrate for OATP1B3. Because severe side effects of FEX were not reported, FEX may be a good probe drug for evaluating the function of OATP1B3 in a clinical situation.

Some reports have indicated that genetic polymorphisms of OATP1B1 affect the pharmacokinetics of pravastatin in vivo (Nishizato et al., 2003;. Mwinyi et al., 2004; Niemi et al., 2004). Therefore, pravastatin can be used as a probe drug for evaluating the function of OATP1B1. Currently, one rare polymorphism in OATP1B3 has been

reported to affect substrate specificities using in vitro analysis (Letschert et al., 2004). However, the impact of the functional change in OATP1B3 by genetic polymorphisms, diseases, and drug-drug interactions on the pharmacokinetics of drugs in humans remains to be clarified, and FEX might be one of the candidate drugs to estimate the OATP1B3 function in vivo.

While this article (manuscript) was under review, Niemi et al. (2005) published the interesting results of a clinical study suggesting that polymorphism in OATP1B1 (T521C), which affected the pharmacokinetics of pravastatin (Nishizato et al., 2003; Mwinyi et al., 2004; Niemi et al., 2004), increased the plasma AUC of fexofenadine. This result appears to conflict with our findings. However, the genetic polymorphism in OATP1B3 was not evaluated in the study by Niemi et al. (2004). The relative importance of OATP1B1 and OATP1B3 in the hepatic uptake of FEX will be determined in larger clinical trials, since the frequency of the polymorphism in OATP1B3 was very low. In addition, specific inhibitors for OATP1B1 and OATP1B3 that can be clinically used will give us a chance to validate our conclusion.

In conclusion, FEX can inhibit both OATP1B1- and OATP1B3-mediated transport, and FEX can be recognized by OATP1B3 preferentially compared with OATP1B1 or OATP2B1. This is the first demonstration that OATP1B3 is thought to be a major transporter involved in the hepatic uptake of FEX.

Acknowledgments. We are grateful to Aventis Pharmaceuticals, Inc. for kindly providing fexofenadine hydrochloride. We thank Masaru Hirano for valuable discussions, Tian Ying and Miyuki Kambara for great assistance with the construction of OATP2B1-expressing cells, and Ayumi Sakai, Keiko Ohsone, and Mika Munemasa for excellent technical assistance.

References

Chu XY, Kato Y, Niinuma K, Sudo KI, Hakusui H, and Sugiyama Y (1997) Multispecific organic anion transporter is responsible for the biliary excretion of the camptothecin derivative irinotecan and its metabolites in rats. *J Pharmacol Exp Ther* **281**:304–314.

Cvetkovic M, Leake B, Fromm MF, Wilkinson GR, and Kim RB (1999) OATP and P-glycoprotein transporters mediate the cellular uptake and excretion of fexofenadine. *Drug Metab Dispos* **27**:866–871.

Dresser GK, Bailey DG, Leake BF, Schwarz UI, Dawson PA, Freeman DJ, and Kim RB (2002) Fruit juices inhibit organic anion transporting polypeptide-mediated drug uptake to decrease the oral availability of fexofenadine. *Clin Pharmacol Ther* **71**:11–20.

Hagenbuch B and Meier PJ (2003) The superfamily of organic anion transporting polypeptides. *Biochim Biophys Acta* **1609**:1–18.

Hagenbuch B and Meier PJ (2004) Organic anion transporting polypeptides of the OATP/SLC21 family: phylogenetic classification as OATP/SLCO superfamily, new nomenclature and molecular/functional properties. *Pflugers Arch* **447**:653–665.

Hamman MA, Bruce MA, Haehner-Daniels BD, and Hall SD (2001) The effect of rifampin administration on the disposition of fexofenadine. *Clin Pharmacol Ther* **69**:114–121.

Hirano M, Maeda K, Shitara Y, and Sugiyama Y (2004) Contribution of OATP2 (OATP1B1) and OATP8 (OATP1B3) to the hepatic uptake of pitavastatin in humans. *J Pharmacol Exp Ther* **311**:139–146.

Hofmann U, Seiler M, Drescher S, and Fromm MF (2002) Determination of fexofenadine in human plasma and urine by liquid chromatography-mass spectrometry. *J Chromatogr B Anal Technol Biomed Life Sci* **766**:227–233.

Ismair MG, Stanca C, Ha HR, Renner EL, Meier PJ, and Kullak-Ublick GA (2003) Interactions of glycyrrhizin with organic anion transporting polypeptides of rat and human liver. *Hepatol Res* **26**:343–347.

Ismair MG, Stieger B, Cattori V, Hagenbuch B, Fried M, Meier PJ, and Kullak-Ublick GA (2001) Hepatic uptake of cholecystokinin octapeptide by organic anion-transporting polypeptides OATP4 and OATP8 of rat and human liver. *Gastroenterology* **121**:1185–1190.

Kobayashi D, Nozawa T, Imai K, Nezu J, Tsuji A, and Tamai I (2003) Involvement of human organic anion transporting polypeptide OATP-B (SLC21A9) in pH-dependent transport across intestinal apical membrane. *J Pharmacol Exp Ther* **306**:703–708.

Konig J, Cui Y, Nies AT, and Keppler D (2000a) A novel human organic anion transporting polypeptide localized to the basolateral hepatocyte membrane. *Am J Physiol* **278**:G156–G164.

Konig J, Cui Y, Nies AT, and Keppler D (2000b) Localization and genomic organization of a new hepatocellular organic anion transporting polypeptide. *J Biol Chem* **275**:23161–23168.

Kullak-Ublick GA, Ismair MG, Stieger B, Landmann L, Huber R, Pizzagalli F, Fattinger K, Meier PJ, and Hagenbuch B (2001) Organic anion-transporting polypeptide B (OATP-B) and its functional comparison with three other OATPs of human liver. *Gastroenterology* **120**:525–533.

Kullak-Ublick GA, Stieger B, and Meier PJ (2004) Enterohepatic bile salt transporters in normal physiology and liver disease. *Gastroenterology* **126**:322–342.

Letschert K, Keppler D, and Konig J (2004) Mutations in the SLCO1B3 gene affecting the substrate specificity of the hepatocellular uptake transporter OATP1B3 (OATP8). *Pharmacogenetics* **14**:441–452.

Lippert C, Ling J, Brown P, and Burmaster S (1996) Mass balance and pharmacokinetics of MDL 16,455A in the healthy, male volunteers. *Pharm Res (NY)* **12**:S-390.

Markham A and Wagstaff AJ (1998) Fexofenadine. *Drugs* 55:269–274; discussion 275–276.

Mwinyi J, Johne A, Bauer S, Roots I, and Gerloff T (2004) Evidence for inverse effects of OATP-C (SLC21A6) 5 and 1b haplotypes on pravastatin kinetics. *Clin Pharmacol Ther* **75**:415–421.

Niemi M, Kivisto KT, Hofmann U, Schwab M, Eichelbaum M, and Fromm MF (2005) Fexofenadine pharmacokinetics are associated with a polymorphism of the *SLCO1B1* gene (encoding OATP1B1). *Br J Clin Pharmacol* **59**:602–604.

Niemi M, Schaeffeler E, Lang T, Fromm MF, Neuvonen M, Kyrklund C, Backman JT, Kerb R, Schwab M, Neuvonen PJ, et al. (2004) High plasma pravastatin concentrations are associated with single nucleotide polymorphisms and haplotypes of organic anion transporting polypeptide-C (OATP-C, SLCO1B1). *Pharmacogenetics* **14**:429–440.

Nishizato Y, Ieiri I, Suzuki H, Kimura M, Kawabata K, Hirota T, Takane H, Irie S, Kusuhara H, Urasaki Y, et al. (2003) Polymorphisms of OATP-C (SLC21A6) and OAT3 (SLC22A8) genes: consequences for pravastatin pharmacokinetics. *Clin Pharmacol Ther* **73**:554–565.

Nozawa T, Imai K, Nezu JI, Tsuji A, and Tamai I (2004) Functional characterization of pH-sensitive organic anion transporting polypeptide OATP-B in human. *J Pharmacol Exp Ther* **308**:438–445.

Pratt CM, Mason J, Russell T, Reynolds R, and Ahlbrandt R (1999) Cardiovascular safety of fexofenadine HCl. *Am J Cardiol* **83**:1451–1454.

Satoh H, Yamashita F, Tsujimoto M, Murakami H, Koyabu N, Ohtani H, and Sawada Y (2005) Citrus juices inhibit the function of human organic anion-transporting polypeptide OATP-B. *Drug Metab Dispos* **33**:518–523.

Simpson K and Jarvis B (2000) Fexofenadine: a review of its use in the management of seasonal allergic rhinitis and chronic idiopathic urticaria. *Drugs* **59**:301–321.

Tannergren C, Knutson T, Knutson L, and Lennernas H (2003) The effect of ketoconazole on the in vivo intestinal permeability of fexofenadine using a regional perfusion technique. *Br J Clin Pharmacol* **55**:182–190.

Yamaoka K, Tanigawara Y, Nakagawa T, and Uno T (1981) A pharmacokinetic analysis program (MULTI) for microcomputer. *J Pharmacobio-Dyn* **4**:879–885.

Address correspondence to: Dr. Yuichi Sugiyama, Department of Molecular Pharmacokinetics, Graduate School of Pharmaceutical Sciences, The University of Tokyo, 7-3-1 Hongo, Bunkyo-ku, Tokyo, 113-0033 Japan. E-mail: sugiyama@mol.f.u-tokyo.ac.jp

Two Common PFIC2 Mutations Are Associated With the Impaired Membrane Trafficking of BSEP/ABCB11

Hisamitsu Hayashi,[1] Tappei Takada,[2] Hiroshi Suzuki,[2] Hidetaka Akita,[3] and Yuichi Sugiyama[1]

Progressive familial intrahepatic cholestasis type 2 (PFIC2) is caused by a mutation in the bile salt export pump (BSEP/ABCB11) gene. However, the mechanisms for the deficiency in the function of two mutations (E297G and D482G), which are frequently found in European patients, have not yet been identified. In the present study, we examined the transport activity and cellular localization of these two mutants in human embryonic kidney 293 and Madin-Darby canine kidney II cells, respectively. Introduction of E297G and D482G mutations into the human BSEP gene by site-directed mutagenesis resulted in a significant reduction in the BSEP expression level, which was associated with impaired membrane trafficking. Most of the D482G BSEP and some of the E297G BSEP underwent only core glycosylation and appeared to be predominantly located in the endoplasmic reticulum. The inhibition of proteasome function by MG132 resulted in the cellular accumulation of the core glycosylation form of the two mutants. In contrast, transport studies for taurocholate and glycocholate with membrane vesicles isolated from complementary DNA–transfected cells indicated that both mutations did not significantly affect the transport function of BSEP *per se*. In conclusion, E297G and D482G mutations result in impaired membrane trafficking, whereas the transport functions of these mutants remain largely unchanged. (HEPATOLOGY 2005;41:916-924.)

The efficient biliary excretion of monovalent bile acids is mediated by the bile salt export pump (BSEP/ABCB11), an ATP-binding cassette transmembrane transporter located on the bile canalicular membrane.[1] The function of BSEP/ABCB11 has been clarified by examining the adenosine triphosphate (ATP)-dependent transport of monovalent bile acids (such as taurocholic acid) in isolated bile canalicular membrane vesicles and/or membrane vesicles isolated from cells transfected with the complementary DNA (cDNA) for BSEP.[2,3]

Many studies have also been performed in patients and it has been shown that the hereditary defect in the expression of BSEP results in the acquisition of progressive familial intrahepatic cholestasis type 2 (PFIC2).[4,5] Genomic analysis of PFIC2 patients has revealed that many kinds of missense, premature termination, frame shift, and splicing junction mutations are associated with the BSEP gene.[4] Among these, E297G and D482G, two missense mutations in the second intracellular loop and in the first ATP-binding domain, respectively, are frequently observed in PFIC2 patients. Indeed, each of these two mutations is present in 30% of European PFIC2 families.[6] Although the presence of the BSEP gene mutations in PFIC2 patients has been demonstrated, little information is available on the mechanism for the association of PFIC2 disease with mutations in the BSEP gene.

Recently, the mechanism for the impaired function of PFIC2-type BSEP was studied by examining the function of mutated rat and mouse Bsep gene products.[7,8] Rat and mouse Bsep genes were used for the analysis because of the difficulties in obtaining human BSEP-expressing cells. It

Abbreviations: PFIC2, progressive familial intrahepatic cholestasis 2; BSEP, bile salt export pump; ATP, adenosine triphosphate; cDNA, complementary DNA; CFTR, cystic fibrosis transmembrane conductance regulator; MRP2, multidrug resistance–associated protein 2; MDCK, Madin-Darby canine kidney; HEK, human embryonic kidney; PCR, polymerase chain reaction; GFP, green fluorescence protein; mRNA, messener RNA; MOI, multiplicity of infection; PBS, phosphate-buffered saline; ER, endoplasmic reticulum.

From the [1]Graduate School of Pharmaceutical Sciences, The University of Tokyo, Hongo, Japan; the [2]Department of Pharmacy, The University of Tokyo Hospital, Faculty of Medicine, The University of Tokyo, Hongo, Japan; and the [3]Graduate School of Pharmaceutical Sciences, Hokkaido University, Sapporo, Japan.

Received July 6, 2004; accepted January 9, 2005.

Supported by a Grant-in-Aid for Scientific Research on Priority Areas Epithelial Vectorial Transport 12144201 from the Ministry of Education, Science, and Culture of Japan.

Address reprint requests to: Yuichi Sugiyama, Ph.D., Professor and Chair, Department of Molecular Biopharmaceutics, Graduate School of Pharmaceutical Sciences, The University of Tokyo, Hongo, Bunkyo-ku, Tokyo 113-0033, Japan. E-mail: sugiyama@mol.f.u-tokyo.ac.jp; fax: (81) 3-5841-4766.

Published online in Wiley InterScience (www.interscience.wiley.com).

DOI 10.1002/hep.20627

Potential conflict of interest: Nothing to report.

was shown that the introduction of some mutations in the consensus region (such as E297G) into the rat and mouse Bsep genes resulted in altered cellular distribution of the Bsep. However, the problem associated with this method is whether or not the function of the mutated rat and mouse Bsep really represents that of mutated human BSEP. In addition, the mechanism remains to be clarified for other important mutations, including D482G, which is very common in European PFIC2 patients.

In the present study, we have examined the mechanism for the pathogenesis of PFIC2 using the mutated human BSEP gene. Previous studies in humans have shown that the concentration of bile acids in the bile is extremely low in PFIC2 patients, and that no BSEP was detectable in the canalicular membrane of some patients.[5] In addition, it has been shown that cystic fibrosis and Dubin-Johnson syndrome are caused by impaired maturation and/or impaired transport function of cystic fibrosis transmembrane conductance regulator (CFTR/ABCC7)[9] and multidrug resistance–associated protein 2 (MRP2/ABCC2),[4,10-13] respectively. Because PFIC2 may also be caused by the same two mechanisms reported for cystic fibrosis and Dubin-Johnson syndrome, we introduced mutations into the human BSEP and examined the cellular localization in Madin-Darby canine kidney (MDCK) II cells, which are commonly used to study the polarized expression of membrane proteins in epithelia. The transport function was determined using isolated membrane vesicles prepared from BSEP cDNA-transfected human embryonic kidney (HEK) 293 cells. We focused particularly on E297G and D482G mutations, which are frequently found in European PFIC2 patients.[6]

Materials and Methods

Materials. [^{3}H]taurocholic acid (2 Ci/mmol) was obtained from NEN Life Science Products (Boston, MA). [^{14}C]glycocholic acid (57.3 mCi/mmol) was purchased from PerkinElmer Life Sciences (Boston, MA). Antibodies against the human BSEP were purchased from Santa Cruz Biotechnology (Santa Cruz, CA). All other chemicals were of analytical grade. HEK 293 and MDCK II cells were cultured in Dulbecco's modified eagle medium (Invitrogen, Carlsbad, CA) supplemented with 10% fetal bovine serum, penicillin (100 U/mL), and streptomycin (100 U/mL) at 37°C with 5% CO_2 and 95% humidity.

Generation of Recombinant Adenovirus. The BSEP cDNA was amplified via polymerase chain reaction (PCR) with Ex-Taq (Takara Bio, Shiga, Japan) from the commercially available cDNA library (Clontech, Palo Alto, CA). Cryptic bacterial promoter was inactivated as previously described[2] before being cloned into the adenovirus shuttle vector pShuttle (Clontech). Construction of the PFIC2 mutants was performed using a QuikChange XL Site-Directed Mutagenesis Kit (Stratagene, La Jolla, CA). The BSEP cDNA was sequenced in an ABI 377 DNA Sequencer (Applied Biosystems, Foster City, CA). The sequence of the wild-type BSEP cDNA was identical to that published (accession number, AF091582).

The cloned wild-type and two mutated cDNAs were introduced into the adenovirus vector (Clontech). The recombinant adenoviruses were produced using the adenovirus expression system, and the titer was checked with an Adeno-X Rapid Titer Kit (Clontech). As a control, recombinant adenoviruses containing green fluorescence protein (GFP) were used.

Determination of BSEP Messenger RNA Levels. For the determination of BSEP messenger RNA (mRNA) levels, MDCK II cells were seeded 24 hours before infection at a density of 1.3×10^6 cells per 10-cm dish and were infected with recombinant adenoviruses containing wild-type, E297G, and D482G BSEP cDNA at a multiplicity of infection (MOI) of 50. RNA was isolated using ISOGEN (Wako Pure Chemical Industries, Osaka, Japan) 48 hours after the infection according to the manufacturer's instructions, and isolated RNA was treated with DNaseI (Takara Shuzo, Tokyo, Japan) at 37°C for 1 hour. Reverse transcription was performed using Oligo dT primer and myeloblastosis virus reverse transcriptase (Takara Shuzo) as previously described.[14] To quantify the expression of mRNA of BSEP in wild-type and mutated BSEP-expressing MDCK II cells, real-time quantitative PCR was performed using a LightCycler and the appropriate software (version 3.53; Roche Diagnostics, Mannheim, Germany). Quantitative PCR was performed using a QuantiTect SYBR Green PCR Kit (Quiagen, Valencia, CA) with 5′-dAGTGGGGGAGCTGAATACAA-3′ and 5′-dCCAATGGTGGCTGCTCCAAT-3′ (BSEP) and 5′-dACTATCGGCAATGAGCGGTTC-3′ and 5′-dAGAGCCACCAATCCACACAGA-3′ (β-actin) as primers. PCR was performed at 94°C for 15 seconds, 55°C for 25 seconds, and 72°C for 20 seconds, which was repeated for 35 cycles. An external standard curve was generated by diluting the target PCR product, which had been purified before use. To confirm amplification specificity, PCR products were subjected to a melting curve analysis and gel electrophoresis. BSEP gene expression in each reaction was normalized by the expression of β-actin.

Detection of BSEP. MDCK II cells were seeded 24 hours before infection at a density of 1.3×10^6 cells per 10-cm dish and were infected with recombinant adenoviruses at 250 MOI. In some instances, to inhibit the activity of proteasomes cells were treated with 5 μmol/L

MG132 (Calbiochem- Novabiochem, San Diego, CA) for 8 hours before preparation of the crude membrane. Crude membrane fractions were prepared 48 hours after infection. The specimens were separated via 7% SDS-PAGE and were subjected to Western blot analysis with a 1,000-fold diluted polyclonal human BSEP antibody as previously described.[15]

To examine BSEP expression on the cell surface, cell surface biotinylation was performed as follows. MDCK II cells were seeded 24 hours before infection in a 12-well plate at a density of 4×10^5 cells per well and were infected with the recombinant adenoviruses at 250 MOI. Cells were washed twice with ice-cold phosphate-buffered saline (PBS) containing 0.1 mmol/L $CaCl_2$ and 1 mmol/L $MgCl_2$ (PBS-Ca/Mg) 48 hours after infection and incubated twice with NHS-SS-biotin (Pierce Biotechnology, Rockford, IL) at 4°C for 30 minutes. After removing the NHS-SS-biotin, the cells were washed with PBS-Ca/Mg containing 100 mmol/L glycine and incubated at 4°C for 15 minutes, then disrupted with 100 μL lysis buffer (50 mmol/L Tris, 150 mmol/L NaCl, 5 mmol/L ethylenediaminetetraacetic acid, 1% Triton-X100 [pH 7.5]) containing 1% SDS and 0.1 mmol/L phenylmethylsulfonyl fluoride at 4°C for 15 minutes. Then, 50 μL aliquots were preserved as whole cell lysate, and the remaining aliquots (50 μL) were diluted with 450 μL lysis buffer containing 1% SDS and 0.1 mmol/L phenylmethylsulfonyl fluoride to reduce the SDS concentration. Streptavidin-agarose beads (Pierce Biotechnology) were then added to the lysate, followed by incubation at 4°C overnight with end-over-end rotation. The beads were washed three times with lysis buffer, twice with high-salt lysis buffer (50 mmol/L Tris, 500 mmol/L NaCl, 5 mmol/L ethylenediaminetetraacetic acid, 0.1 % Triton-X 100 [pH 7.5]), and once with low-salt lysis buffer (50 mmol/L Tris [pH 7.5]). The biotinylated proteins were eluted with 30 μL 3 × SDS loading buffer (Biolabs, Hertfordshire, UK) diluted to 1 × SDS with PBS at 60°C for 5 minutes. The biotinylated proteins (30 μL) and total cell lysate (30 μL) were subjected to Western blot analysis.

To examine the extent of glycosylation of BSEP, peptide N-glycosidase F (New England Biolabs, Beverly, MA) digestions were performed at 37°C for 2 hours as described by the manufacturer. The deglycosylated proteins were subjected to Western blot analysis.

Immunofluorescence. To determine the localization of BSEP, MDCK II cells were seeded on glass coverslips 24 hours before infection at a density of 3×10^5 cells/well in 12-well plates and were infected with recombinant adenoviruses at 25 MOI (wild-type and E297G BSEP) or 250 MOI (D482G BSEP). Cells were fixed with 100% methanol at −20°C for 10 minutes 48 hours after the infection, and were permeabilized in 1% Triton X-100 (Sigma, St. Louis, MO) in PBS for 5 minutes. After permeabilization, cells were incubated with 100-fold diluted polyclonal human BSEP antibodies at 4°C for 16 hours and then with 250-fold diluted Alexa Flour 488 donkey anti-goat immunoglobulin G at room temperature for 1 hour. Confocal laser scanning was performed using an LSM 510 apparatus (Carl Zeiss, Oberkochen, Germany).

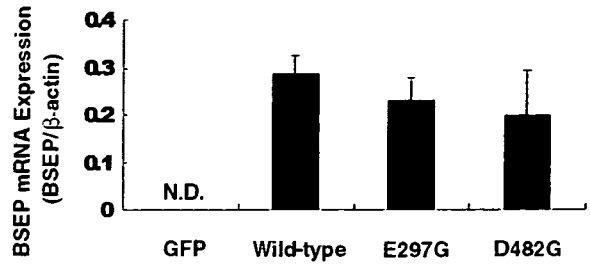

Fig. 1. Determination of expression levels of BSEP mRNA. RNA was isolated from MDCK II cells 48 hours after infection by recombinant adenoviruses at 50 MOI. Real-time quantitative PCR was performed as described in Materials and Methods. BSEP gene expression in each reaction was normalized by the expression of β-actin. Horizontal bars represent the mean ± SE of triplicate determinations. BSEP, bile salt export pump; mRNA, messener RNA; N.D., not detected; GFP, green fluorescence protein.

Transport Assays. To determine the transport function of BSEP, HEK 293 cells were seeded 72 hours before infection at a density of 4.0×10^6 cells per 15-cm dish and were infected with recombinant human BSEP adenovirus at 25 MOI. Crude membrane fractions[16] and isolated membrane vesicles[14] were prepared 48 hours after infection as previously described.[14,16] Prepared crude membrane fractions and isolated membrane vesicles were subjected to Western blot analysis. Transport assays were performed using the rapid filtration method previously reported.[14]

Results

Expression of Wild-Type and Two Mutated BSEP in MDCK II Cells. To examine the cellular localization and transport function of the two mutants (E297G and D482G), we constructed recombinant adenoviruses containing wild-type and mutated BSEP cDNA. Expression of BSEP mRNA in the infected MDCK II cells was confirmed via quantitative PCR (Fig. 1). BSEP gene expression was normalized by the expression of β-actin. It was found that the BSEP mRNA expression levels were similar between the wild-type and the two mutants.

The expression level of BSEP was further examined via Western blot analysis (Fig. 2A). It was found that the expression levels of these two mutants were lower than

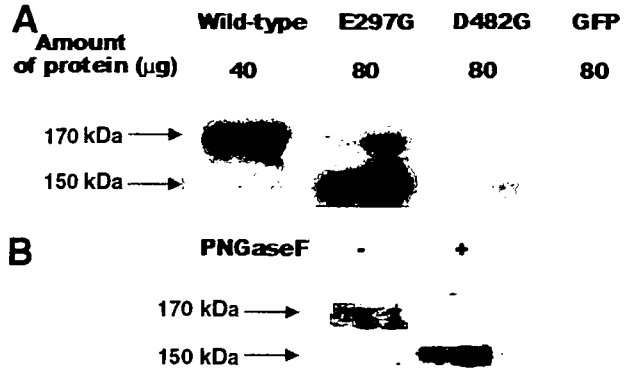

Fig. 2. Determination of expression levels of BSEP. The expression level of BSEP was determined via Western blot analysis. (A) Results of Western blot analysis with crude membrane fraction prepared from MDCK II cells. MDCK II cells were infected with recombinant adrenoviruses at 250 MOI 48 hours before the experiments. Crude membrane fractions prepared from GFP (control), wild-type, E297G, and D482G BSEP-expressing MDCK II cells (80, 40, 80, and 80 μg protein, respectively) were analyzed. (B) Results of Western blot analysis of crude membrane fraction (40 μg protein) expressing wild-type BSEP before and after peptide N-glycosidase F digestion. GFP, green fluorescence protein.

that of the wild-type BSEP. Although the wild-type BSEP was detected as approximately 170 kDa, D482G BSEP was detected as approximately 150 kDa. In addition, E297G BSEP was detected as approximately 170 kDa and approximately 150 kDa bands. Treatment of wild-type BSEP with peptide N-glycosidase F, which is able to cleave the high mannose- and complex-type sugar chains, resulted in the appearance of a band at approximately 150 kDa (Fig. 2B). These results suggest that D482G BSEP and some of the E297G BSEP molecules are present as immature endoplasmic reticulum (ER)-resident forms.

Cellular Localization of Wild-Type and Two Mutated BSEP in MDCK II Cells. We then examined the cellular localization of wild-type and mutated BSEP in MDCK II cells using the immunofluorescence and cell surface biotinylation methods. Although wild-type BSEP is predominantly localized in the apical membrane at 25 MOI (Fig. 3A), there was very little expression of D482G BSEP in most cells at 25 MOI because of the low expression level, as suggested by Western blot analysis (see Fig. 2A). An increase in the MOI to 250 resulted in significant expression of D482G BSEP, suggesting that D482G BSEP are expressed intracellularly (see Fig. 3A). E297G BSEP was located in both the intracellular compartment and apical membrane at 25 MOI (see Fig. 3A). Typical images from the immunofluorescence study are shown in Fig. 3A. To avoid any selection bias, the immunofluorescence study was performed three times, and many fields were selected in each experiment; we obtained the same results in all experiments (see Fig. 3A).

Furthermore, we examined the cell surface expression of wild-type and mutated BSEP via biotinylation assay in MDCK II cells. Cell surface BSEP was detected in wild-type and E297G-expressing MDCK II cells as the mature form, whereas no D482G BSEP molecules were detectable on the cell surface (Fig. 3B). This result is also consistent with the results of the Western blot analysis of the whole cell lysate in which the mature form of D482G BSEP was not detectable (see Fig. 3B).

Proteasome-Mediated Degradation of Two Mutants. It has been reported that proteasomes play an important role in the degradation of incompletely folded and misfolded protein retained in the ER.[17,18] Because the expression levels of E297G and D482G BSEP were lower than that of the wild-type BSEP—and because it is possible that these mutants are localized in the ER—proteasomes may be responsible for their degradation. To examine this hypothesis, cells were treated with 5 μmol/L MG132, a specific proteasome inhibitor, for 8 hours, and its effects on E297G and D482G BSEP were examined via Western blot anasysis. Western blot analysis showed that MG132 treatment caused the accumulation of immature forms (150 kDa), particularly in E297G and D482G BSEP–expressing MDCK II cells (Fig. 4). These results were also consistent with those obtained via immunofluorescence studies. It was found that MG132 treatment resulted in an increase in the number of wild-type, E297G, and D482G BSEP–expressing cells, and the degree of increase was particularly high for the latter two; in the absence of MG132, the number of E297G BSEP-expressing cells after adenovirus infection was only approximately 25% of those expressing wild-type BSEP, and only a minimal number of cells expressed D482G BSEP. In contrast, in the presence of MG132, the number of cells expressing E297G and D482G BSEP was almost the same as that in wild-type BSEP-expressing cells after infection of adenoviruses at the same MOI (data not shown). In the presence of MG132, E297G and D482G BSEP were predominantly expressed in the intracellular compartment, which is the same as that observed under control conditions (see Fig. 3A). This suggests that the expression level of BSEP is increased by MG132, resulting in an increase in the number of cells, the BSEP expression of which was visualized in the immunofluorescence studies.

Transport Function of Wild-Type and Two Mutated BSEP. The transport function of wild-type and mutated BSEP was studied by examining the ATP-dependent uptake of [^{3}H]taurocholate and [^{14}C]glycocholate into membrane vesicles isolated from HEK 293 cells that were infected with recombinant adenoviruses. Although inside-out membrane vesicles—the ATP-hydrolysis re-

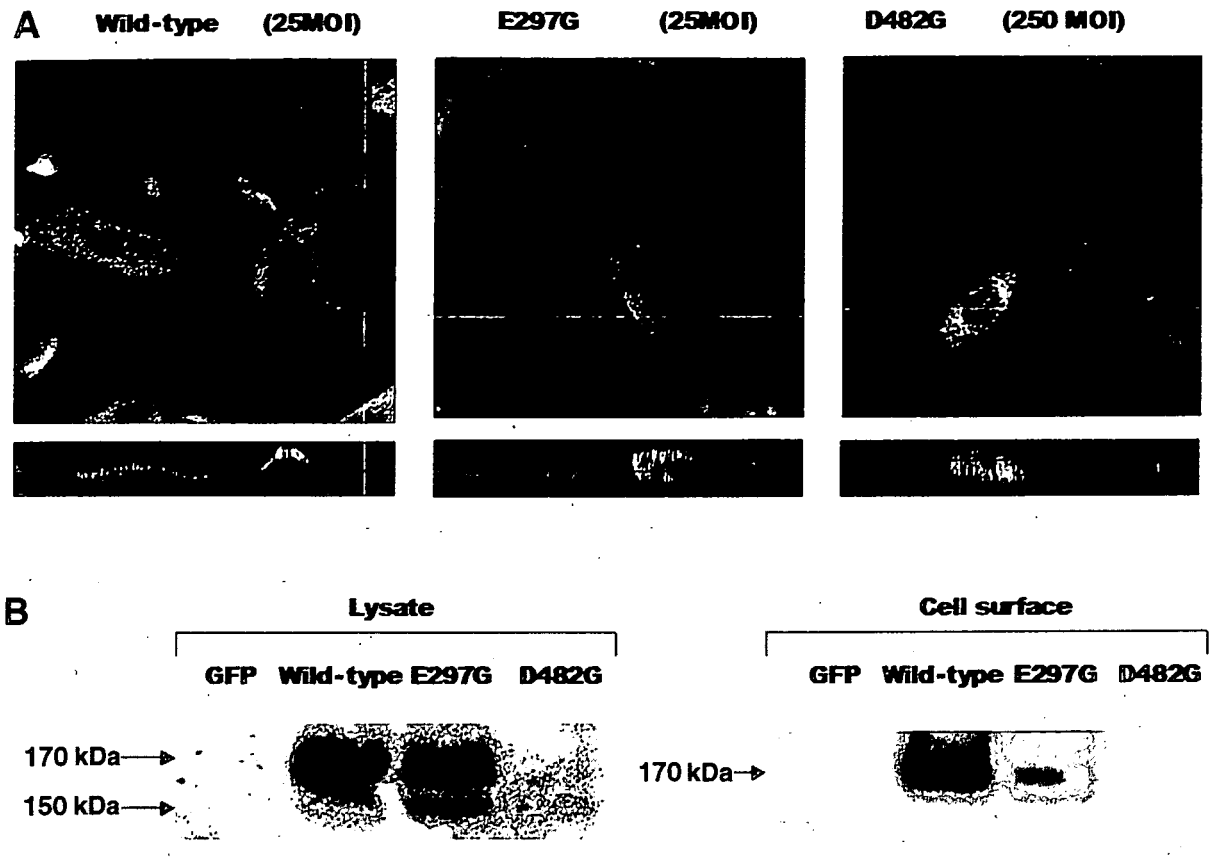

Fig. 3. Localization of BSEP in MDCK II cells. MDCK II cells expressing wild-type and mutated BSEP were analyzed to determine the cellular localization of BSEP by confocal laser scanning microscopy and cell surface biotinylation analysis. (A) Typical results of confocal laser scanning microscopy. MDCK II cells were infected with the recombinant adenoviruses at 25 MOI (wild-type and E297G BSEP) or 250 MOI (D482G BSEP) 48 hours before the experiments. Green and red fluorescence represent BSEP and nuclei, respectively. In each panel, the upper section shows the *en face* image and the lower section shows the vertical image. (B) Results of biotinylation analysis. MDCK II cells were infected with recombinant adenoviruses at 250 MOI 48 hours before the experiments. The cell surface fractions were prepared using the biotinylation method as described in Materials and Methods. The whole cell lysate and biotinylated proteins were subjected to Western blot analysis. MOI, multiplicity of infection; GFP, green fluorescence protein.

gion of which faces to the outside of membrane vesicles—are required to evaluate ATP-dependent transport, it is difficult to prepare inside-out membrane vesicles from MDCK II cells. Consequently, the transport function was studied using isolated membrane vesicles from HEK 293 cells.

Before the transport experiments, the expression level of BSEP was compared among the isolated membrane vesicles expressing wild-type, E297G, and D482G BSEP. D482G BSEP, as well as wild-type and E297G BSEP, were detected as approximately 170-kDa bands in isolated membrane vesicles (Fig. 5A). The band density of the 170-kDa form of E297G and D482G in the isolated membrane vesicles was approximately 25% and 10% of wild-type BSEP, respectively (Fig. 5B). In addition, the degree of expression of the 170-kDa form in the isolated membrane vesicles was twofold higher than that in the crude membrane fractions (Fig. 5C).

The ATP-dependent uptake of taurocholate and glycocholate by wild-type, E297G and D482G BSEP–expressing isolated membrane vesicles was much higher than that by GFP-expressing vesicles (Fig. 6A). By normalizing the BSEP expression levels in the isolated membrane vesicles based on the results of Western blot analysis (see Fig. 5B), it was demonstrated that the transport of taurocholate and glycocholate mediated per unit mass of E297G and D482G BSEP molecules was not significantly different from that by wild-type BSEP (Figs. 5B and 6B). We also performed a kinetic analysis to examine the effect of the two mutations on the transport function of BSEP. Wild-type, E297G, and D482G BSEP–mediated initial ATP-dependent uptake rates were saturable with apparent K_m values of 4.61 ± 0.91, 5.41 ± 0.27, and 14.3 ± 2.0 μmol/L, respectively (Fig. 6C). The maximum taurocholate transport velocity (V_{max}) for wild-type, E297G, and D482G BSEP were 2310 ± 220, 485 ± 15, and 761 ± 60 pmol/min/mg isolated membrane vesicle protein, respectively. By considering the expression level of BSEP in the isolated membrane vesicles (see Fig. 5B), the maximum transport velocity per unit

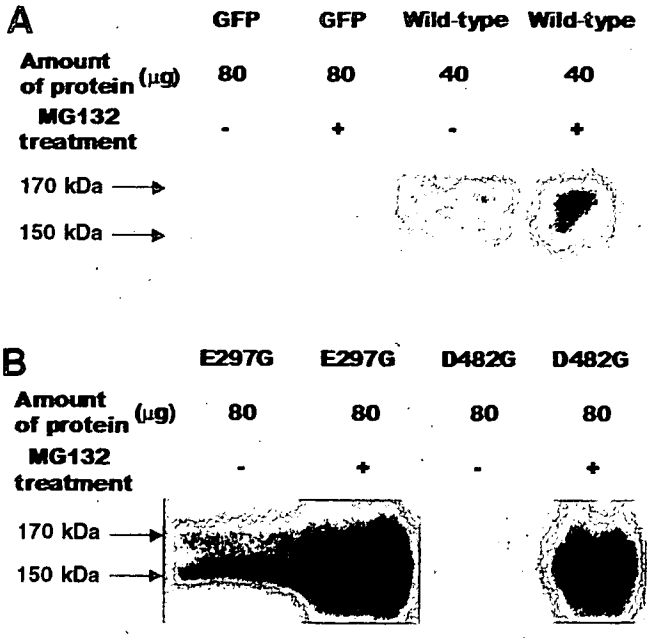

Fig. 4. Effects of proteasome inhibitors on the localization of BSEP in MDCK II cells. MDCK II cells were infected with recombinant adenoviruses at 250 MOI 48 hours before the experiments. Crude membrane fractions prepared from GFP (control), wild-type, E297G, and D482G BSEP-expressing MDCK II cells (80, 40, 80, and 80 μg protein, respectively), treated with or without 5 μmol/L MG132 for 8 hours before the preparation of crude membrane, were subjected to Western blot analysis. GFP, green fluorescence protein.

mass of E297G and D482G BSEP molecules was calculated to be 94% and 329%, respectively, of wild-type BSEP.

Discussion

In the present study, we analyzed the consequence of two frequently found PFIC2 mutations (E297G and D482G) *in vitro* to investigate the pathogenesis of PFIC2. Initially, we examined mRNA and protein levels of wild-type and two mutated BSEP. Although quantitative PCR showed no difference in mRNA levels between the wild-type and two mutated BSEP (see Fig. 1), Western blot analysis indicated reduced expression of D482G and E297G BSEP (see Fig. 2A). In addition, the molecular weight of most of the D482G BSEP and some of the E297G molecules was approximately 150 kDa (see Fig. 2A). Together with the finding that peptide N-glycosidase F treatment of wild-type BSEP results in the appearance of a band at approximately 150 kDa (see Fig. 2B), this suggests that these two mutated BSEP molecules are present as the immature and core-glycosylated form. The absence of glycosylation is consistent with the hypothesis that these mutants are trapped in the ER and are not transferred to the Golgi apparatus where the glycosylation takes place. This suggestion is also consistent with the immunofluorescence observations which indicated that D482G and E297G BSEP molecules are located intracellularly (see Fig. 3A). The results of the surface biotinylation study also suggested that the D482G BSEP and core glycosylated form of E297G BSEP are located intracellularly (see Fig. 3B). In addition, the results of the MG132 treatment experiment suggested that E297G and D482G BSEP molecules are degraded by the proteasome pathway (see Fig. 4). It is possible that the mutated BSEP molecules are degraded by the proteasome pathway after being trapped in the ER, as has been suggested for CFTR ΔF508[17,19] and some MRP2 mutants.[10-12] The impaired BSEP function in PFIC2 patients may also be accounted for by this mechanism. Although the immunohistochemical studies indicate a loss of BSEP on the canalicular membrane in PFIC2 patients with the E297G mutation, we found that some E297G BSEP with a molecular mass of approximately 170 kDa were expressed on the apical membrane (see Fig. 3B). At the present moment, we do not know the reason why some E297G BSEP molecules are trafficked in a normal manner. It is possible that the capacity of the degradation pathway may be saturated due to the high transient expression of BSEP by the adenovirus expression system and, consequently, some of the mutated BSEP molecules are trafficked to the apical membrane. Alternatively, it is also possible that the reduction in the expression level on the apical membrane of E297G BSEP (approximately 25% of wild-type BSEP; see Fig. 3B) may be related to the pathogenesis of PFIC2.

We have also examined the transport function of mutated BSEP using membrane vesicles isolated from HEK 293 cells infected with recombinant adenoviruses. Western blot analysis of the isolated membrane vesicles indicated the presence of approximately 170-kDa molecules for wild-type, E297G, and D482G BSEP. Moreover, it was found that the amount of 150-kDa molecules for E297G and D482G BSEP in the isolated membrane vesicles was lower than that in the crude membrane fraction. It is possible that the isolated membrane vesicles are enriched with the plasma membrane, rather than the membrane fractions from the intracellular compartment. The enrichment of the plasma membrane in the isolated membrane vesicles was confirmed by examining the activity of γ-glutamyltranspeptidase, a plasma membrane marker enzyme. The activity in the isolated membrane vesicles was 1.77 ± 0.60 times higher than that in the crude membrane fraction. This result is consistent with the results of the Western blot analysis, which indicated that the band density of the 170-kDa form of BSEP in the isolated membrane vesicle was approximately twice that in the crude membrane fraction (see Fig. 5C).

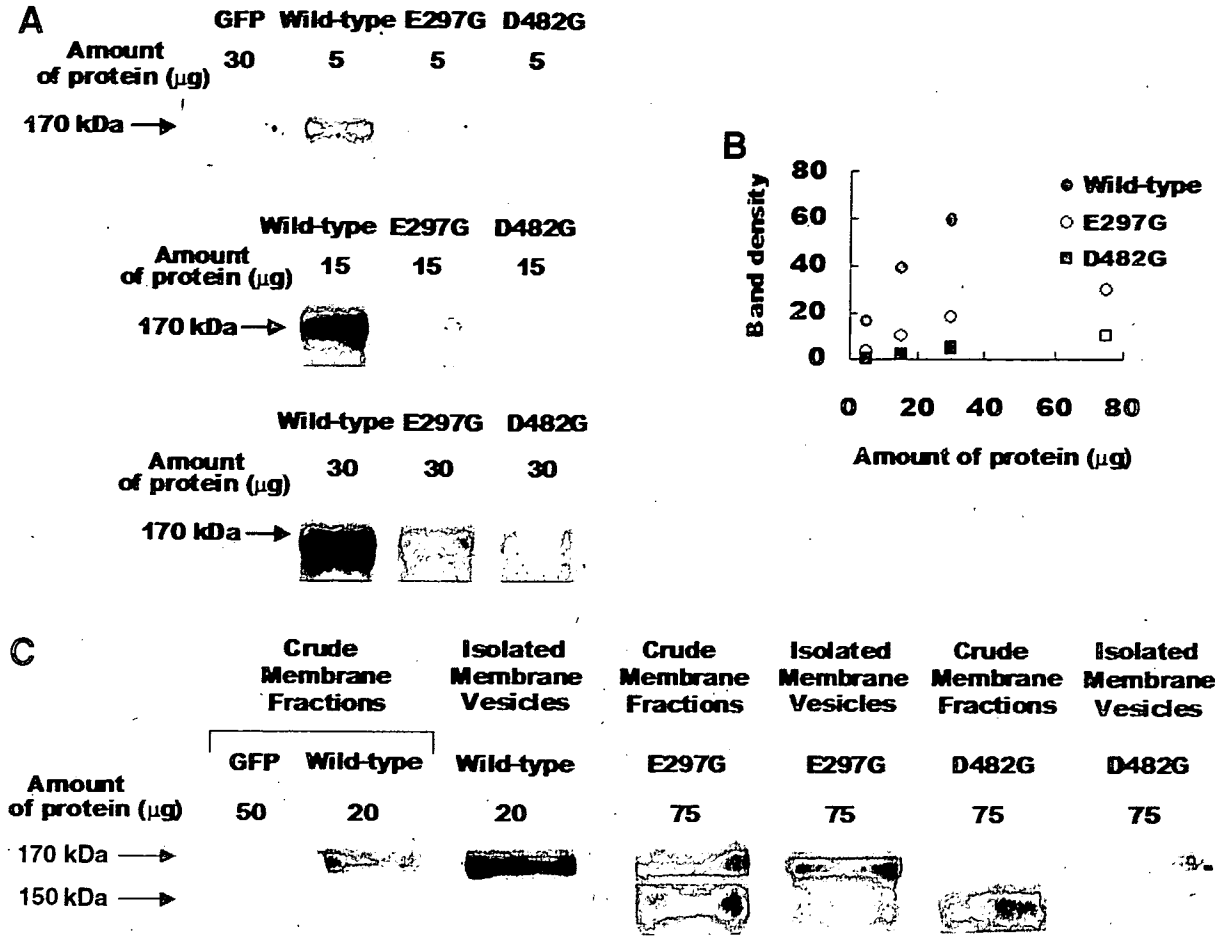

Fig. 5. Expression level of BSEP in isolated membrane vesicles. The expression level of BSEP in isolated membrane vesicles was determined via Western blot analysis. HEK 293 cells were infected with recombinant adrenoviruses at 25 MOI 48 hours before to the experiments. (A) Results of Western blot analysis with isolated membrane vesicles prepared from HEK 293 cells. 5 μg (upper lane), 15 μg (middle lane) and 30 μg (lower lane) protein of isolated membrane vesicles prepared from GFP (control), wild-type, E297G and D482G BSEP-expressing HEK 293 cells were subjected to Western blot analysis. (B) Relationship between the applied amount and the band density. The results for wild-type (●), E297G (○), and D482G (■) BSEP are shown. (C) Results of Western blot analysis using crude membrane fraction and isolated membrane vesicles prepared from GFP (control), wild-type, E297G, and D482G BSEP-expressing HEK 293 cells (50, 20, 75, and 75 μg protein, respectively). GFP, green fluorescence protein.

Functional analysis using these membrane vesicles indicated that the transport of taurocholate and glycocholate in E297G and D482G BSEP–expressing isolated membrane vesicles was significantly higher than that in control isolated membrane vesicles (see Fig. 6A). Based on the hypothesis that the transport activity per unit mass of BSEP molecules can be calculated by considering the BSEP expression level in the isolated membrane vesicles, it was found that the transport of taurocholate and glycocholate mediated per unit mass of E297G and D482G BSEP molecules was not reduced compared with wild-type BSEP (see Figs. 5B and 6B). The K_m values for taurocholate of wild-type, E297G, and D482G BSEP molecules were consistent with previous observations obtained using membrane vesicles isolated from human wild-type BSEP cDNA-infected Sf9 and Sf High Five cells.[2,3] Based on these results, it appears that the transport function of two mutated BSEP molecules (E297G and D482G) *per se* remains normal (see Fig. 6). These results suggest that, if E297G and D482G are matured and consequently expressed on the membrane surface, these mutated transporters are able to transport BSEP substrates.

Our results using mutated human BSEP were different from those reported in a previous study, in which the cause of PFIC2 was examined using mutated rat Bsep,[7] but they were consistent with those reported recently, in which the effect of D482G mutation was examined using mouse Bsep.[8] In the study using rat Bsep gene, the pathogenic mechanism for the D482G mutation was not identified because D482G rat Bsep is localized in the apical membrane as well as the cytoplasm of MDCK cells, and this mutation did not significantly affect taurocholate transport examined using

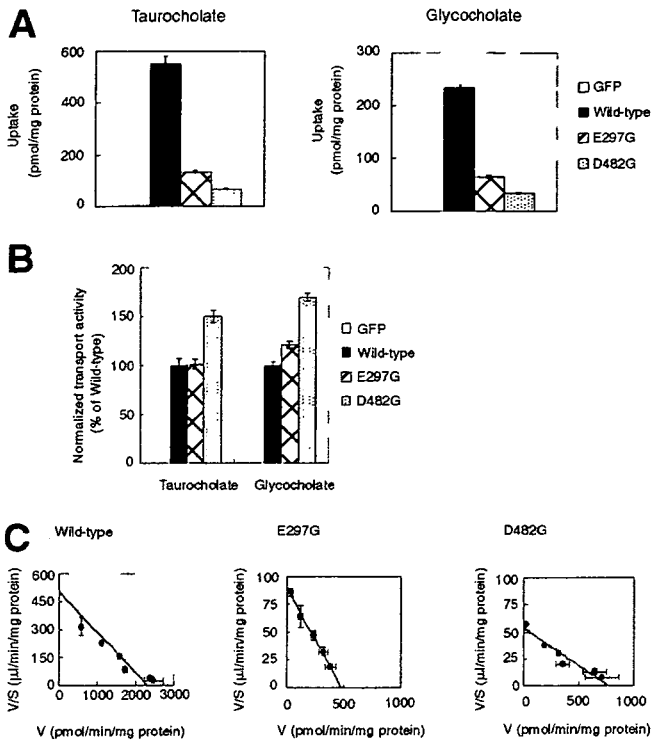

Fig. 6. Transport function of BSEP. Transport function of BSEP was determined using isolated membrane vesicles. HEK 293 cells were infected with recombinant adrenoviruses at 25 MOI 48 hours before the experiments. (A) Uptake of taurocholate (1 μmol/L) and glycocholate (2 μmol/L) into 5 μg protein of isolated membrane vesicles. The isolated membrane vesicles prepared from HEK 293 cells expressing GFP (control) (**white bars**), wild-type (**black bars**), E297G (**cross-hatched bars**), and D482G BSEP (**dotted bars**) were incubated at 37°C for 2 minutes with 5 mmol/L ATP or AMP. The uptake of ligand was obtained by subtracting the value in the absence of ATP from that in its presence. (B) Normalized uptake of taurocholate and glycocholate. The transport activity shown in panel A was normalized by the BSEP expression level shown in Fig. 5B. (C) Saturation of the uptake of taurocholate by the isolated membrane vesicles. The uptake of [^{3}H]taurocholate was examined in the presence and absence of 1.5 to 100 μmol/L of unlabeled taurocholate. Other experimental conditions are described in panel A. Results are given as the Eadie-Hofstee plot for wild-type and mutated BSEP. Each point and vertical/horizontal bar represents the mean ± SE of triplicate determinations. GFP, green fluorescence protein.

membrane vesicles isolated from Sf9 cells.[7] In contrast, in the study with mouse Bsep gene, it was found that D482G mutation resulted in impaired canalicular trafficking in HepG2 cells, although this mutation did not affect the transport of taurocholate examined using membrane vesicles isolated from Sf21 cells.[8] Concerning E297G mutation, it has been shown that E297G rat Bsep is widely distributed throughout the cytoplasm, and the studies using isolated membrane vesicles indicated that this mutation resulted in the loss of taurocholate transport activity.[7] The differences among these results involving the previous mutated rat Bsep, mouse Bsep, and the present mutated human BSEP may be explained by considering the species difference in the Bsep/BSEP sequence, although the homology of the amino acid sequence around E297G and D482G is quite high as far as human BSEP and rat and mouse Bsep are concerned. For example, it is still possible that the introduction of the D482G mutation to human BSEP, but not rat Bsep, results in a conformational change in human BSEP so that D482G BSEP is bound to some molecular chaperons.

The features of D482G BSEP resemble those of the CFTR ΔF508 mutant in that the deletion of phenylalanine at 508 results in the accumulation of the mutated protein in the ER followed by proteasome degradation. In addition, CFTR ΔF508 can transport chloride ions[20] if the mutated transporter is expressed on the plasma membrane. One of the methods being explored as a potential treatment of CFTR ΔF508 patients is to administer drugs (such as sodium 4-phenylbutyrate) which are capable of trafficking the mutated protein to the apical membrane by inhibiting the binding to the molecular chaperons in the ER.[21-23] After clarifying the mechanism for the intracellular retention of E297G and D482G BSEP, it is possible to identify agents able to target these mutated BSEP molecules to the apical surface. Because both of the mutated BSEP molecules *per se* are associated with normal transport functions, it may be possible to treat these PFIC2 patients with such agents.

In conclusion, the results of the present *in vitro* study suggest that E297G and D482G, which are frequently observed PFIC2 mutations, cause deficient BSEP maturation, although the transport functions of these mutants *per se* remain almost normal. These pieces of information should be useful in understanding the pathogenesis of PFIC2.

References

1. Gerloff T, Stieger B, Hagenbuch B, Madon J, Landmann L, Roth J, et al. The sister of P-glycoprotein represents the canalicular bile salt export pump of mammalian liver. J Biol Chem 1998;273:10046-10050.
2. Noe J, Stieger B, Meier PJ. Functional expression of the canalicular bile salt export pump of human liver. Gastroenterology 2002;123:1659-1666.
3. Byrne JA, Strautnieks SS, Mieli-Vergani G, Higgins CF, Linton KJ, Thompson RJ. The human bile salt export pump: characterization of substrate specificity and identification of inhibitors. Gastroenterology 2002; 123:1649-1658.
4. Strautnieks SS, Bull LN, Knisely AS, Kocoshis SA, Dahl N, Arnell H, et al. A gene encoding a liver-specific ABC transporter is mutated in progressive familial intrahepatic cholestasis. Nat Genet 1998;20:233-238.
5. Jansen PL, Strautnieks SS, Jacquemin E, Hadchouel M, Sokal EM, Hooiveld GJ, et al. Hepatocanalicular bile salt export pump deficiency in patients with progressive familial intrahepatic cholestasis. Gastroenterology 1999;117:1370-1379.
6. Thompson R, Strautnieks S. BSEP: function and role in progressive familial intrahepatic cholestasis. Semin Liver Dis 2001;21:545-550.
7. Wang L, Soroka CJ, Boyer JL. The role of bile salt export pump mutations in progressive familial intrahepatic cholestasis type II. J Clin Invest 2002; 110:965-972.
8. Plass JR, Mol O, Heegsma J, Geuken M, de Bruin J, Elling G, et al. A progressive familial intrahepatic cholestasis type 2 mutation causes an un-

stable, temperature-sensitive bile salt export pump. J Hepatol 2004;40:24-30.
9. Cheng SH, Gregory RJ, Marshall J, Paul S, Souza DW, White GA, et al. Defective intracellular transport and processing of CFTR is the molecular basis of most cystic fibrosis. Cell 1990;63:827-834.
10. Keitel V, Nies AT, Brom M, Hummel-Eisenbeiss J, Spring H, Keppler D. A common Dubin-Johnson syndrome mutation impairs protein maturation and transport activity of MRP2 (ABCC2). Am J Physiol Gastrointest Liver Physiol 2003;284:G165-174.
11. Keitel V, Kartenbeck J, Nies AT, Spring H, Brom M, Keppler D. Impaired protein maturation of the conjugate export pump multidrug resistance protein 2 as a consequence of a deletion mutation in Dubin-Johnson syndrome. HEPATOLOGY 2000;32:1317-1328.
12. Hashimoto K, Uchiumi T, Konno T, Ebihara T, Nakamura T, Wada M, et al. Trafficking and functional defects by mutations of the ATP-binding domains in MRP2 in patients with Dubin-Johnson syndrome. HEPATOLOGY 2002;36:1236-1245.
13. Mor-Cohen R, Zivelin A, Rosenberg N, Shani M, Muallem S, Seligsohn U. Identification and functional analysis of two novel mutations in the multidrug resistance protein 2 gene in Israeli patients with Dubin-Johnson syndrome. J Biol Chem 2001;276:36923-36930.
14. Akita H, Suzuki H, Ito K, Kinoshita S, Sato N, Takikawa H, et al. Characterization of bile acid transport mediated by multidrug resistance associated protein 2 and bile salt export pump. Biochim Biophys Acta 2001; 1511:7-16.
15. Suzuki M, Suzuki H, Sugimoto Y, Sugiyama Y. ABCG2 transports sulfated conjugates of steroids and xenobiotics. J Biol Chem 2003;278: 22644-22649.
16. Sasaki M, Suzuki H, Ito K, Abe T, Sugiyama Y. Transcellular transport of organic anions across a double-transfected Madin-Darby canine kidney II cell monolayer expressing both human organic anion-transporting polypeptide (OATP2/SLC21A6) and multidrug resistance-associated protein 2 (MRP2/ABCC2). J Biol Chem 2002;277:6497-6503.
17. Ward CL, Omura S, Kopito RR. Degradation of CFTR by the ubiquitin-proteasome pathway. Cell 1995;83:121-127.
18. Kopito RR. ER quality control: the cytoplasmic connection. Cell 1997;88: 427-430.
19. Gelman MS, Kannegaard ES, Kopito RR. A principal role for the proteasome in endoplasmic reticulum-associated degradation of misfolded intracellular cystic fibrosis transmembrane conductance regulator. J Biol Chem 2002;277:11709-11714.
20. Li C, Ramjeesingh M, Reyes E, Jensen T, Chang X, Rommens JM, et al. The cystic fibrosis mutation (delta F508) does not influence the chloride channel activity of CFTR. Nat Genet 1993;3:311-316.
21. Jiang C, Fang SL, Xiao YF, O'Connor SP, Nadler SG, Lee DW, et al. Partial restoration of cAMP-stimulated CFTR chloride channel activity in DeltaF508 cells by deoxyspergualin. Am J Physiol 1998;275:C171-178.
22. Rubenstein RC, Egan ME, Zeitlin PL. In vitro pharmacologic restoration of CFTR-mediated chloride transport with sodium 4-phenylbutyrate in cystic fibrosis epithelial cells containing delta F508-CFTR. J Clin Invest 1997;100:2457-2465.
23. Rubenstein RC, Zeitlin PL. A pilot clinical trial of oral sodium 4-phenylbutyrate (Buphenyl) in deltaF508-homozygous cystic fibrosis patients: partial restoration of nasal epithelial CFTR function. Am J Respir Crit Care Med 1998;157:484-490.

Available online at www.sciencedirect.com
SCIENCE DIRECT
Biochimica et Biophysica Acta 1738 (2005) 54 – 62
BIOCHIMICA ET BIOPHYSICA ACTA
BBA
http://www.elsevier.com/locate/bba

Transport by vesicles of glycine- and taurine-conjugated bile salts and taurolithocholate 3-sulfate: A comparison of human BSEP with rat Bsep

Hisamitsu Hayashi [a], Tappei Takada [b], Hiroshi Suzuki [b], Reiko Onuki [a], Alan F. Hofmann [c], Yuichi Sugiyama [a,*]

[a] *Department of Molecular Biopharmaceutics, Graduate School of Pharmaceutical Sciences, The University of Tokyo, 7-3-1 Hongo, Bunkyo-ku, Tokyo 113-0033, Japan*
[b] *Department of Pharmacy, The University of Tokyo Hospital, Faculty of Medicine, The University of Tokyo, Hongo, Japan*
[c] *Department of Medicine, University of California, San Diego, CA 92093-0813, USA*

Received 13 July 2005; received in revised form 17 October 2005; accepted 25 October 2005
Available online 15 November 2005

Abstract

The bile salt export pump (BSEP) of hepatocyte secretes conjugated bile salts across the canalicular membrane in an ATP-dependent manner. The biliary bile salts of human differ from those of rat in containing a greater proportion of glycine conjugates and taurolithocholate 3-sulfate (TLC-S). In the present study, the transport properties of hBSEP and rBsep were investigated using membrane vesicles from HEK293 cells infected with recombinant adenoviruses containing hBSEP or rBsep cDNA. ATP-dependent uptake of radiolabeled glycine-, taurine-conjugated bile salts, and [^{3}H]cholate was observed when hBSEP or rBsep was expressed. Comparison of initial uptake rates indicated that for both transporters, taurine-conjugated bile salts were transported more rapidly than glycine-conjugated bile salts, however, hBSEP transported glycine conjugates to an extent that was approximately 2-fold greater than rBsep. In addition, [^{3}H]TLC-S was significantly transported by hBSEP, and hardly transported by rBsep. The mean K_m value for the uptake of [^{3}H]TLC-S by hBSEP was 9.5 ± 1.5 μM, a value similar to that for hMRP2 (8.2 ± 1.3 μM). In conclusion, both hBSEP and rBsep transport taurine-conjugated bile salts better than glycine-conjugated bile salts, but hBSEP transports glycine conjugates to a greater extent as compared to rBsep. TLC-S, which is present in human bile but not rodent bile, is more avidly transported by hBSEP compared with rBsep.

Keywords: Bile salt; ABC transporter; hBSEP/rBsep

1. Introduction

Bile formation is one of important functions of the liver. Vectorial transport of bile salts from the sinusoidal space to the canaliculus via hepatocytes provides an osmotic driving force for bile formation [1,2]. Transport of bile salts across the sinusoidal membrane is mediated at least in part by both Na^+-taurocholate co-transporting polypeptide (human NTCP/SLC10A1 and rat Ntcp/Slc10a1) [3,4] and Na^+-independent organic anion transporting polypeptides (human OATP/SLCO and rat Oatp/Slco) [1,2]. After reaching the canalicular membrane, monovalent taurine- and glycine-conjugated bile salts are secreted into bile by the bile salt export pump (human BSEP/ABCB11 and rat Bsep/Abcb11) [5–10], whereas sulfated bile salt amidates and bile salt ethereal glucuronides (divalent) are excreted by the multidrug resis-

Abbreviations: BSEP/Bsep, human/rat isoforms of the bile salt export pump; hMRP2/rMrp2, human/rat isoforms of multidrug resistance associated protein 2; hNTCP/rNtcp, human/rat isoforms of Na^+-taurocholate co-transporting polypeptide; hOATP/rOatp, human/rat isoforms of organic anion transporting polypeptide; HEK293, human embryonic kidney 293; PFIC, progressive familial intrahepatic cholestasis; DJS, Dubin-Johnson syndrome; MOI, multiplicity of infection; GFP, green fluorescent protein; TC, taurocholate; GC, glycocholate; CA, cholate; TCDC, taurochenodeoxycholate; GCDC, glycochenodeoxycholate; CDCA, chenodeoxycholate; TUDC, tauroursodeoxycholate; GUDC, glycoursodeoxycholate; UDCA, ursodeoxycholate; TDC, taurodeoxycholate; LCA, lithocholate; TLC-S, taurolithocholate 3-sulfate

* Corresponding author. Tel.: +81 3 5841 4770; fax: +81 3 5841 4766.
E-mail address: sugiyama@mol.f.u-tokyo.ac.jp (Y. Sugiyama).

1388-1981/$ - see front matter © 2005 Elsevier B.V. All rights reserved.
doi:10.1016/j.bbalip.2005.10.006

tance associated protein 2 (human MRP2/ABCC2 and rat Mrp2/Abcc2) [11–13].

The transport properties of hBSEP/rBsep and hMRP2/rMrp2 have been clarified recently. The function of hBSEP/rBsep has been characterized by examining the ATP-dependent transport of taurine- and glycine-conjugated bile salts in isolated bile canalicular membrane vesicles (CMVs) and/or membrane vesicles isolated from hBSEP/rBsep-expressing cells [5–8]. For hMRP2/rMrp2, the transport characteristics have been mainly investigated by comparing transport across the bile canalicular membrane in normal rats with that in Mrp2-deficient rats [8,14–16]. Mutations in BSEP gene are now known to be the cause of progressive familial intrahepatic cholestasis type 2 (PFIC2) [17–21], whereas mutations in MRP2 are the cause of Dubin–Johnson syndrome (DJS) [22–24].

Major bile salts in mammals, i.e., ionized forms of C24-bile acids, are synthesized from cholesterol in the liver and then conjugated (N-acylamidated) with glycine or taurine. In health, sulfation of primary bile salts does not occur in most mammals, but in cholestasis at least in some species, bile salts are extensively sulfated and eliminated into urine. The biliary bile salt composition in the human significantly differs from that in the rat. In humans, the majority of bile salts are conjugated with glycine, whereas in rats, most bile salts are conjugated with taurine. Human bile, but not rat bile, contains sulfated and unsulfated amidates of lithocholate (LCA) [25,26].

Two groups have attempted to relate the transport properties of hBSEP to biliary bile salt composition in humans as compared to that in rats [5,7]. Noe et al. concluded that the transport property of hBSEP/rBsep does not explain the differences in steady state biliary bile salt composition between the two species, because of the similarity of K_m value and intrinsic clearance value for TC, GC, TCDC and TUDC [7]. On the other hand, Byrne et al. concluded that the transport properties of hBSEP/rBsep do in fact correlate with the different bile salt pools in human and rat due to the difference of the relative affinities for TC, GC, TCDC and GCDC between hBSEP and rBsep [5]. In the present study, we have characterized the transport function of hBSEP and rBsep for twelve physiologic bile salts including several kinds of bile salts untested in the previous reports, such as taurolithocholate 3-sulfate. The transport function was determined using membrane vesicles from HEK293 cells infected with recombinant adenoviruses containing hBSEP and rBsep cDNA. We were able to confirm that the transport properties of hBSEP/rBsep reflect the difference in bile salt composition between human and rat. Kinetic analyses to hBSEP and hMRP2 were also performed for [^{3}H]TLC-S, since the initial uptake study demonstrated that this sulfated bile salt is good substrate for hBSEP, not good substrate for rBsep.

2. Materials and methods

2.1. Materials and cell culture

[^{3}H]cholate (CA) (24.5 Ci/mmol), [^{3}H]taurocholate (TC) (2 Ci/mmol), [^{14}C]chenodeoxycholate (CDCA) (48.6 mCi/mmol) and [2-^{3}H]taurine (30.3 Ci/mmol) were purchased from NEN Life Sciences Products (Boston, MA). [^{14}C]glycocholate (GC) (57.3 mCi/mmol) and [^{14}C]lithocholate (LCA) (57.3 mCi/mmol) were purchased from American Radiolabeled Chemicals, Inc. (St. Louis, MO). [^{3}H]ursodeoxycholate (UDCA) (20 Ci/mmol), [^{3}H]tauroursodeoxycholate (TUDC) (10 Ci/mmol), [^{3}H]glycoursodeoxycholate (GUDC) (11 Ci/mmol), [^{3}H]taurochenodeoxycholate (TCDC) (10 Ci/mmol), [^{3}H]glycochenodeoxycholate (GCDC) (11 Ci/mmol) and [^{3}H]taurodeoxycholate (TDC) (29 Ci/mmol) were synthesized in the laboratory of Alan F. Hofmann as described elsewhere [27]. The tritium label was at C-22 and C-23 and has been shown to be stable during hepatocyte transport [28]. [^{3}H]TLC-S was synthesized from lithocholate 3-sulfate using [2-^{3}H]taurine (30.3 Ci/mmol) as described previously [16]. Unlabeled UDCA, TUDC and GUDC were kindly provided by Mitsubishi Pharma (Osaka, Japan). All other chemicals used were commercially available and of reagent grade.

Antiserum for rBsep was raised in rabbits against an oligopeptide (the carboxyl terminal of rBsep; AYYKLVITGAPIS) [29].

Human embryonic kidney (HEK) 293 cells were cultured in Dulbecco's modified Eagle medium (Invitrogen, Carlsbad, CA) supplemented with 10% FBS, penicillin (100 U/ml) and streptomycin (100 U/ml) at 37 °C with 5% CO_2 and 95% humidity.

2.2. Generation of recombinant adenovirus

Full-length hBSEP, rBsep, and hMRP2 cDNAs were cloned as described previously [17,29,30]. The cloned hBSEP, rBsep and hMRP2 cDNAs were introduced into Adeno-X™ viral DNA (Clontech, Palo Alto, CA). The recombinant adenoviruses were produced using the adenovirus expression system according to the manufacturer's instructions, and the titer was examined by an Adeno-X Rapid Titer Kit (Clontech). As a control, recombinant adenoviruses containing green fluorescence protein (GFP) were used.

2.3. Transport studies with membrane vesicles

In order to determine the transport function of hBSEP, rBsep and hMRP2, HEK293 cells were seeded 72 h before infection at a density of 4.0×10^6 cells per 15 cm dish, and infected with recombinant adenovirus at 25 MOI. The isolated membrane vesicles were prepared 48 h after infection as described previously [17]. Transport assays were performed using the rapid filtration method as reported previously [17].

2.4. Western blot analysis

The isolated membrane vesicles were prepared as described above and dissolved in 3 × SDS sample buffer (New England BioLabs, Beverly, MA). The specimens were separated on a 7% SDS-PAGE, and subjected to Western blot analysis with a 1000-fold diluted anti-rBSEP serum as described previously [17].

3. Results

3.1. Uptake of [^{3}H]TC into membrane vesicles

The expression of hBSEP or rBsep in the membrane vesicles prepared from the transfected HEK293 cells was confirmed by Western blot analysis (Fig. 1). As shown in

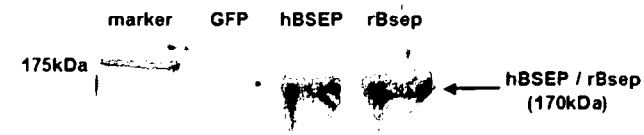

Fig. 1. Western blot analysis of hBSEP and rBsep. Membrane vesicles (15 μg) isolated from hBSEP-, rBsep- and GFP-transfected HEK293 cells were separated on a 7% SDS-PAGE. The proteins transferred to the polyvinylidene difluoride membrane by electroblotting were detected by polyclonal anti-rBsep antiserum.

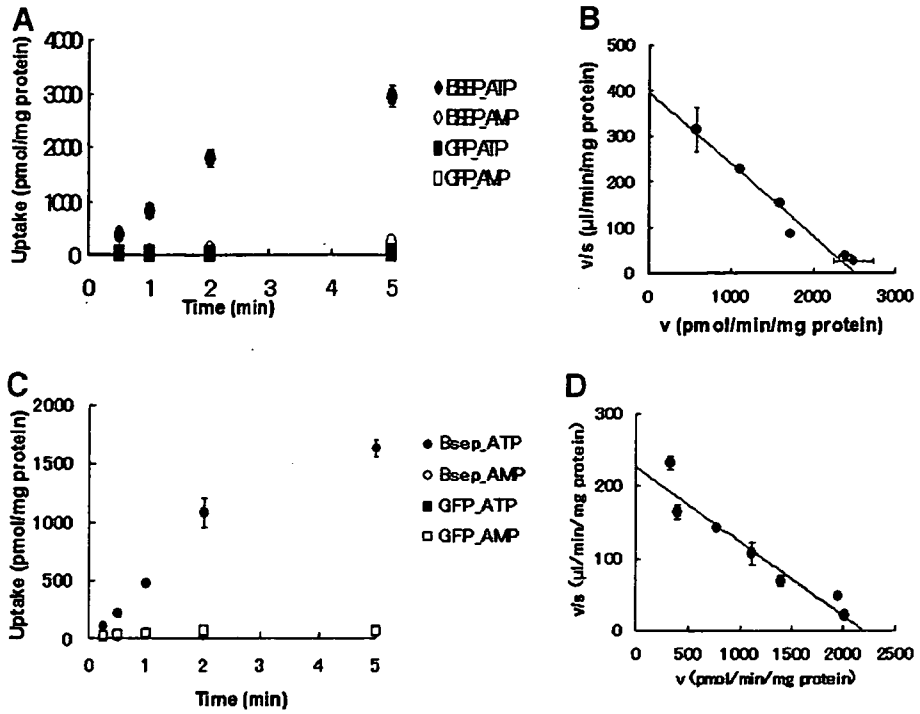

Fig. 2. Uptake of [^{3}H]TC by hBSEP and rBsep. A and C show the time profile for the hBSEP-mediated (A) and rBsep-mediated (C) uptake of [^{3}H]TC. Membrane vesicles (5 μg) prepared from hBSEP-transfected (circles), rBsep-transfected (circles) and GFP-transfected (squares) HEK293 cells were incubated at 37 °C with 5 mM ATP (closed symbols) or AMP (open symbols) in medium containing 0.8 μM [^{3}H]TC and 1.2 μM TC. B and D show the saturation of the hBSEP-mediated (B) and rBsep-mediated (D) uptake of [^{3}H]TC. The uptake of 0.8 μM [^{3}H]TC by hBSEP- and rBsep-expressing membrane vesicles (5 μg) was determined at 37 °C for 2 min with 5 mM ATP or AMP in medium containing 1.5–100 μM of TC. The ATP-dependent uptake was obtained by subtracting the values in the absence of 5 mM ATP from those in the presence of ATP. Results are shown as in an Eadie–Hofstee plot. The solid line represents the fitted line obtained by non-linear regression analysis. Each point and bar represents the mean ± S.E. of triplicate determinations.

Fig. 1, hBSEP and rBsep were detected as an approximately 170 kDa form in the fraction of membrane vesicles prepared from hBSEP- and rBsep-transfected HEK 293 cells. No expression of hBSEP or rBsep was detected in the control membrane vesicles prepared from GFP-transfected HEK293 cells.

The time-profiles for the uptake of [^{3}H]TC into the membrane vesicles are shown in Fig. 2A and C. The ATP-dependent uptake of [^{3}H]TC into the membrane vesicles markedly depended on the expression of hBSEP and rBsep. Compared with GFP-transfected HEK 293 cells, the uptake of [^{3}H]TC was linear up to 2 min and was 238-fold and 128-fold higher at 2 min in hBSEP- and rBsep-transfected HEK293 cells, respectively.

A kinetic analysis revealed that the ATP-dependent uptake of [^{3}H]TC into hBSEP-expressing membrane vesicles could be described by a single saturable component with $K_m = 6.2 \pm 0.7$ μM and $V_{max} = 2510 \pm 220$ pmol/min/mg protein. For rBsep, values were $K_m = 9.7 \pm 1.3$ μM and $V_{max} = 2200 \pm 110$ pmol/min/mg protein (Fig. 2B and D).

3.2. Uptake of a series of bile salts into membrane vesicles

In addition to TC uptake, the uptake of a variety of natural conjugated and unconjugated bile salts into membrane vesicles was characterized for the purpose of examining the difference between hBSEP and rBsep. The hBSEP- and rBsep-expressing membrane vesicles showed significant ATP-dependent uptake for radiolabeled taurine- and glycine-conjugated bile salts and [^{3}H]CA, whereas radiolabeled unconjugated bile salts, except for [^{3}H]CA, were not transported by hBSEP and rBsep (Fig. 3A and B). Of interest, [^{3}H]TLC-S was ATP-dependently transported by hBSEP, but hardly transported by rBsep (Fig. 3A and B). The initial velocity for hBSEP- and rBsep-mediated uptake of bile salts was in the following order, TCDC > GCDC > TDC ≒ TUDC > TC > GUDC > TLC-S > GC > CA in hBSEP, TCDC > GCDC ≒ TDC ≒ TUDC ≒ TC > GUDC > GC > CA ≒ TLC-S in rBsep (Fig. 3A and B). For both hBSEP and rBsep, conjugates of CDCA were transported more rapidly than conjugates of CA. In addition, both species transported taurine-conjugated bile salts to a greater extent than glycine-conjugated bile salts.

A comparison of the initial ATP-dependent uptake of a series of bile salts by hBSEP- and rBsep-expressing membrane vesicles is shown in Fig. 4. The values for ATP-dependent uptake rate by hBSEP and rBsep expression as compared with that of GFP control were calculated from Fig. 3A and B. Then, the ATP-dependent uptake for each bile salt by hBSEP and rBsep was normalized to that for [^{3}H]TC by hBSEP and rBsep, respectively (Fig. 4). This figure demonstrates the greater transport of hBSEP for glycine-conjugated bile salts as compared to rBsep, consistent with preferential glycine amidation of bile salts in humans as compared to preferential taurine amidation in rats.

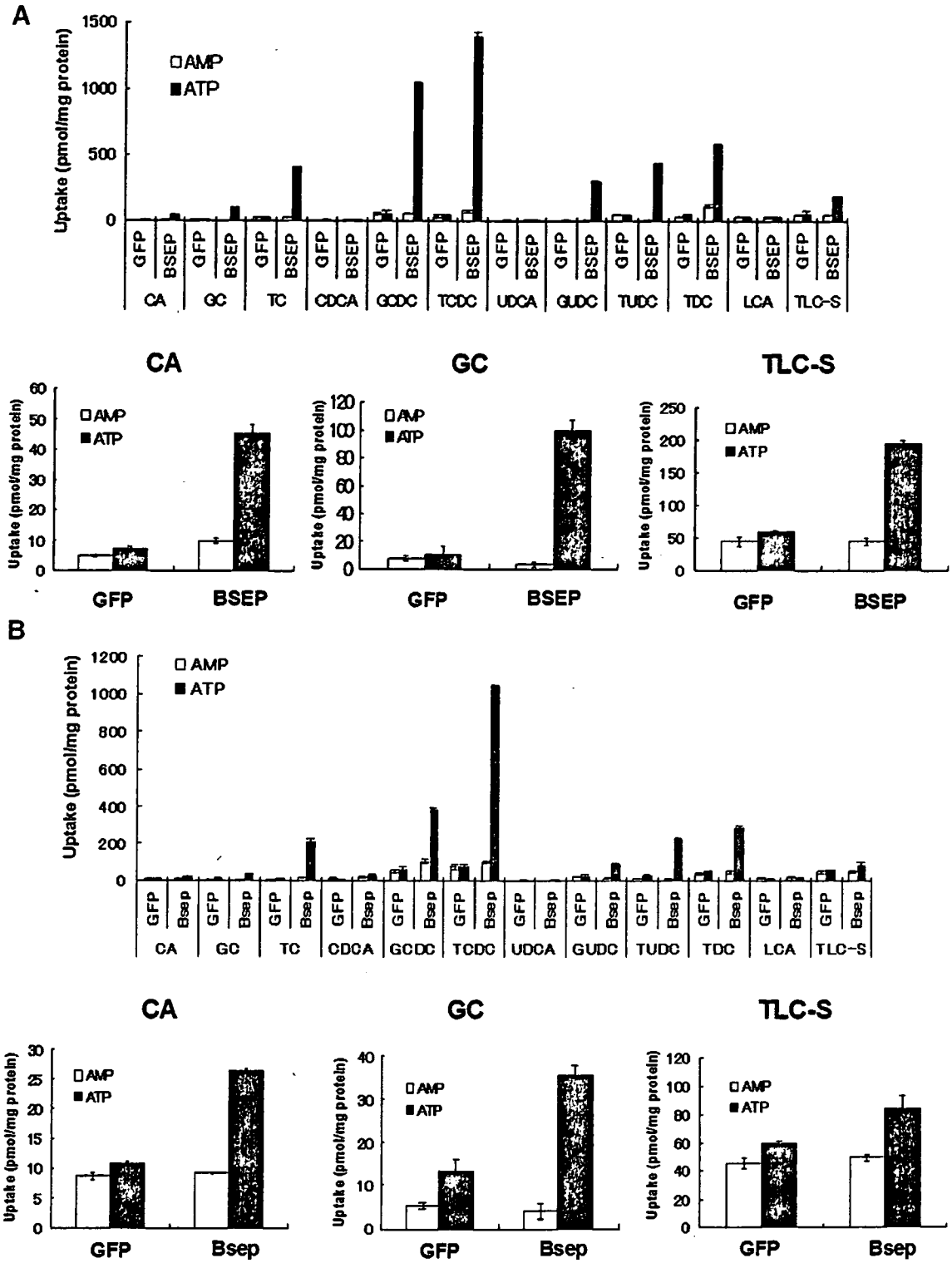

Fig. 3. Initial uptake of a series of bile salts by hBSEP and rBsep. Membrane vesicles (5 μg) prepared from hBSEP-transfected (A), rBsep-transfected (B) and GFP-transfected HEK293 cells were incubated at 37 °C for 30 s with 5 mM ATP (closed columns) or AMP (open columns) in medium containing 2 μM [^{3}H]CA, [^{14}C]GC, [^{3}H]TC, [^{14}C]CDCA, [^{3}H]GCDC, [^{3}H]TCDC, [^{3}H]UDCA, [^{3}H]GUDC, [^{3}H]TUDC, [^{3}H]TDC, [^{14}C]LCA and [^{3}H]TLC-S. Each column and vertical bar represents the mean ± S.E. of triplicate determinations.

Since a species difference was observed for the transport properties of TCDC, GCDC and GC, we performed a kinetic analysis to further characterize the hBSEP- and rBsep-mediated transport of GC, TCDC and GCDC. Like [^{3}H]TC, the ATP-dependent uptake of [^{14}C]GC, [^{3}H]TCDC and [^{3}H]GCDC into hBSEP- and rBsep-expressing membrane vesicles could be described by a single saturable component. The K_m and intrinsic clearance values (V_{max}/K_m) are summarized in the

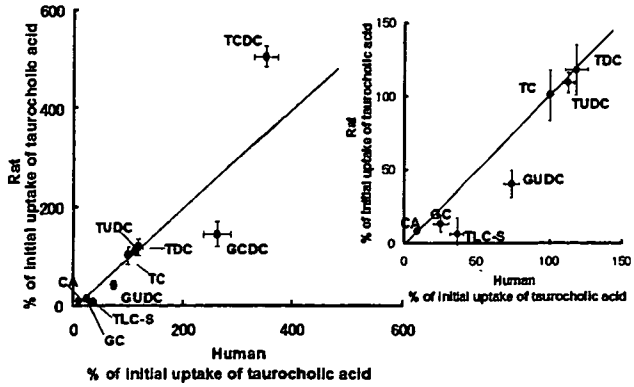

Fig. 4. Comparison of the initial ATP-dependent uptake of a series of bile salts by hBSEP and rBsep. Mean values for the initial ATP-dependent uptake of a series of bile salts (2 μM) by hBSEP and rBsep for 30 s were cited from Fig. 3. The ATP-dependent uptake was obtained by subtracting the values in the absence of 5 mM ATP from those in the presence of ATP. The ATP-dependent uptake for each bile salt by hBSEP and rBsep was normalized with respect to that for TC by hBSEP and rBsep, respectively. Each point and bar represents the mean ± S.E. of triplicate determinations.

Table 1. When the transport rates were expressed as intrinsic clearance values (V_{max}/K_m), the rank order of the extent of the transport rates was TCDC>GCDC>TC>GC in hBSEP and TCDC>GCDC≒TC>GC in rBsep. For the K_m values, no species difference was observed.

3.3. Transport kinetics of [^{3}H]TLC-S

The species difference for TLC-S transport was confirmed by examining the inhibitory effect of TLC-S on the ATP-dependent uptake of [^{3}H]TC by hBSEP- and rBsep-expressing membrane vesicles. The uptake of [^{3}H]TC was inhibited by TLC-S in a concentration-dependent manner with an IC_{50} of 9.0±0.9 μM for hBSEP. For rBsep, the IC_{50} was 52.9±7.9 μM (Fig. 5). The IC_{50} value of TLC-S for [^{3}H]TC uptake by rBsep was comparable with that from our previous study using rBsep-expressing Sf9 membrane vesicles (61.9±19.6 μM) [16].

Transport studies involving [^{3}H]TLC-S using hMRP2-expressing membrane vesicles as well as those using hBSEP-expressing membrane vesicles were performed to compare the affinity of hBSEP for TLC-S with that of hMRP2 which is responsible for the biliary excretion of TLC-S [13,31]. The time-profiles for the uptake of [^{3}H]TLC-S into the membrane vesicles are shown in Fig. 6A and C. There was a marked ATP-dependent uptake of [^{3}H]TLC-S into the membrane vesicles when either hBSEP or hMRP2 was expressed. Compared with GFP-transfected HEK 293 cells, the ATP-dependent uptake of [^{3}H]TLC-S was linear up to 2 min and was 6.2-fold and 5.1-fold higher at 2 min in hBSEP- and hMRP2-transfected HEK293 cells.

A kinetic analysis revealed that the ATP-dependent uptake of [^{3}H]TLC-S into hBSEP- and hMRP2-expressing membrane vesicles could be described by a single saturable component with K_m=9.5±1.5 μM and V_{max}=2100±170 pmol/min/mg protein for hBSEP. For hMRP2, values were K_m=8.2±1.3 μM and V_{max}=1530±120 pmol/min/mg protein (Fig. 6B and D).

4. Discussion

In the present study, we compared the transport properties of hBSEP and rBsep using membrane vesicles from HEK293 cells infected with adenoviruses containing these cDNAs. Our aim was to examine the correlation between the function of hBSEP/rBsep and the biliary bile salt composition.

Initially, transport studies were performed by measuring the ATP-dependent uptake of [^{3}H]TC into the hBSEP- and rBsep-expressing membrane vesicles to confirm the transport function of hBSEP and rBsep. The K_m values for the hBSEP and rBsep mediated transport of [^{3}H]TC calculated by kinetic analysis were 6.2 μM and 9.7 μM, respectively (Fig. 2). These values are comparable with the previously reported values determined in membrane vesicles from hBSEP- and rBsep-expressing Sf9 cells (4.2 μM [5] and 7.9 μM [7] for hBSEP, 5.3 μM [6] and 7.5 μM [16] for rBsep), and in CMVs (4.2 μM [32] for human and 2.1 μM [33] for rat).

In order to investigate the transport properties of hBSEP and rBsep, we also examined the ATP-dependent uptake of another eleven physiological bile salts, including the bile salts untested in previous reports, by hBSEP and rBsep. Significant ATP-dependent uptake of radiolabeled glycine-, taurine-conjugated bile salts and [^{3}H]CA into hBSEP- and rBsep-expressing membrane vesicles was observed (Fig. 3). rBsep transports [^{3}H]TLC-S less avidly compared with hBSEP (Fig. 3A and B). The rank order determined by the initial velocity (hBSEP: TCDC>GCDC>TDC≒TUDC>TC>GUDC>TLC-S>GC>CA, rBsep: TCDC>GCDC≒TC≒TDC≒TUDC>GUDC>GC>CA≒TLC-S) (Fig. 3) was identical to that given by intrinsic clearance values (V_{max}/K_m) using K_m and V_{max} values calculated by kinetic analysis (hBSEP: TCDC>GCDC>TC>GC, rBsep: TCDC>GCDC≒TC>GC) (Table 1). These results agree closely with the previous studies which showed that the rank orders for the intrinsic clearance values of hBSEP and the initial velocity of rBsep were TCDC>TC>TUDC>GC >> CA≒0 [7] and TCDC>GCDC>TC>TDC≒TUDC>GC [8], respectively. The only major difference between the findings of present study and those of the previous study [7] is that CA was not transported by hBSEP in the previous study using membrane vesicles from Sf9 cells. A possible explanation is that the high expression of hBSEP and rBsep by the adenovirus expression

Table 1
Comparison of K_m and V_{max}/K_m values between hBSEP and rBsep

	hBSEP		rBsep	
	K_m (μM)	V_{max}/K_m (μl/min/mg protein)	K_m (μM)	V_{max}/K_m (μl/min/mg protein)
TC	6.2±0.7	400±60	9.7±1.3	230±30
GC	21.7±4.4	78±19	25.7±4.2	47±10
TCDC	6.6±1.2	1300±250	10.2±2.3	820±200
GCDC	7.5±1.0	1000±190	5.6±0.5	240±20

The K_m and V_{max} values for TC were determined by non-linear regression analysis using the data shown in Fig. 2. The K_m and V_{max} values for GC, TCDC, GCDC were determined by the same procedure as that for TC.